THESIS

DEVELOPMENT OF A COMBUSTION SYSTEM FOR FECAL MATERIALS

Submitted by

Maxwell Flagge

Department of Mechanical Engineering

In partial fulfillment of the requirements

For the Degree of Master of Science

Colorado State University

Fort Collins, Colorado

Summer 2017

Master's Committee:

    Advisor: Anthony Marchese

    John Mizia
    Shantanu Jathar
    Sheryl Magzamen

ABSTRACT

DEVELOPMENT OF A COMBUSTION SYSTEM FOR FECAL MATERIALS

CSU is working with Research Triangle Institute on the Reinvent the Toilet Challenge (RTTC) to develop a fecal matter combustion system. The proposed system will dry, pelletize and combust fecal matter from a community bathroom in a net zero energy consumption process. This technology has the potential to reduce disease by improving sanitation in rural villages that lack modern plumbing.

This research is aimed at helping the 2.5 billion individuals in the world who lack modern plumbing and sanitation facilities. Many villages have nothing more than a concrete pit for defecation, and some individuals have no alternative to open defecation, which creates a huge potential for disease transmission. If individuals could safely burn away their fecal material without using any external energy or resources, the instances of sanitation-related disease could be greatly reduced.

In this project, CSU's primary tasks are the optimization and automation of fecal combustion technology. The current combustor design is a modified continuous feed downdraft gasifier. Through a series of tests and measurements, several modifications and improvements have been made to the combustor and its control system, allowing the system to burn fecal materials cleanly and efficiently, while ensuring the destruction of any disease-causing pathogens or bacteria.

TABLE OF CONTENTS

LIST OF FIGURES

CHAPTER 1: OVERVIEW

1.1 Reinvent the Toilet Challenge

The Bill and Melinda Gates foundation launched the Reinvent the Toilet Challenge (RTTC) in 2011. This initiative is aimed at bringing "sustainable sanitation solutions to the 2.5 billion people worldwide who don't have access to safe, affordable sanitation" [1]. The challenge requires a sanitation system that destroys disease-causing pathogens and bacteria in fecal material while recovering resources from the waste (namely energy, water, and nutrients). The sanitation system must operate without any infrastructure (no electrical or water hookups), and cost less than five cents per user, per day.

The Colorado State University (CSU) cookstoves research team was contracted by Research Triangle Institute (RTI) to create a modern high-efficiency combustor to sanitize waste as part of a full sanitation (toilet) system. The processes involved in the sanitation system include separation of solid and liquid waste streams, drying of solid fecal material, burning of dried fecal material, and electrolysis of liquid waste. The separation of waste streams allows for a more efficient drying process, and simultaneous liquid/solid sanitation. The drying of solid fecal material occurs at a high enough temperature (at or above 150°C) to kill any disease-causing bacteria (e.g. helminths, *E.coli*, etc.). The dried fecal material can then be burned to dispose of the solid waste while leaving behind a small amount of ash. Electrolysis of the liquid waste stream removes any inorganic compounds from the wastewater, and produces sanitized non-potable water. A team at Duke University was contracted by RTI to help design and test the urine sanitation system.

1.2 Fecal Combustion

When investigated by L. Yermán *et al.* the content of fresh fecal material (75-85%) necessitated the use of "substantial pre-drying or the use of supplemental fuel" to allow the fuel's pyrolysis to be self-sustaining [2]. The combustion system must, therefore, include a drying sequence that can effectively dehydrate fecal material before they are burned. Jetter *et al*. found gasifiers to have "notably low emissions" in comparison to all other cookstove technologies [3]. In addition, from previous cookstoves work conducted at CSU different biomass cookstove technologies, we see that gasification tends to produce less particulate matter and carbon monoxide than other technologies. A general guide for different cookstove emissions can be seen below in Figure 1.
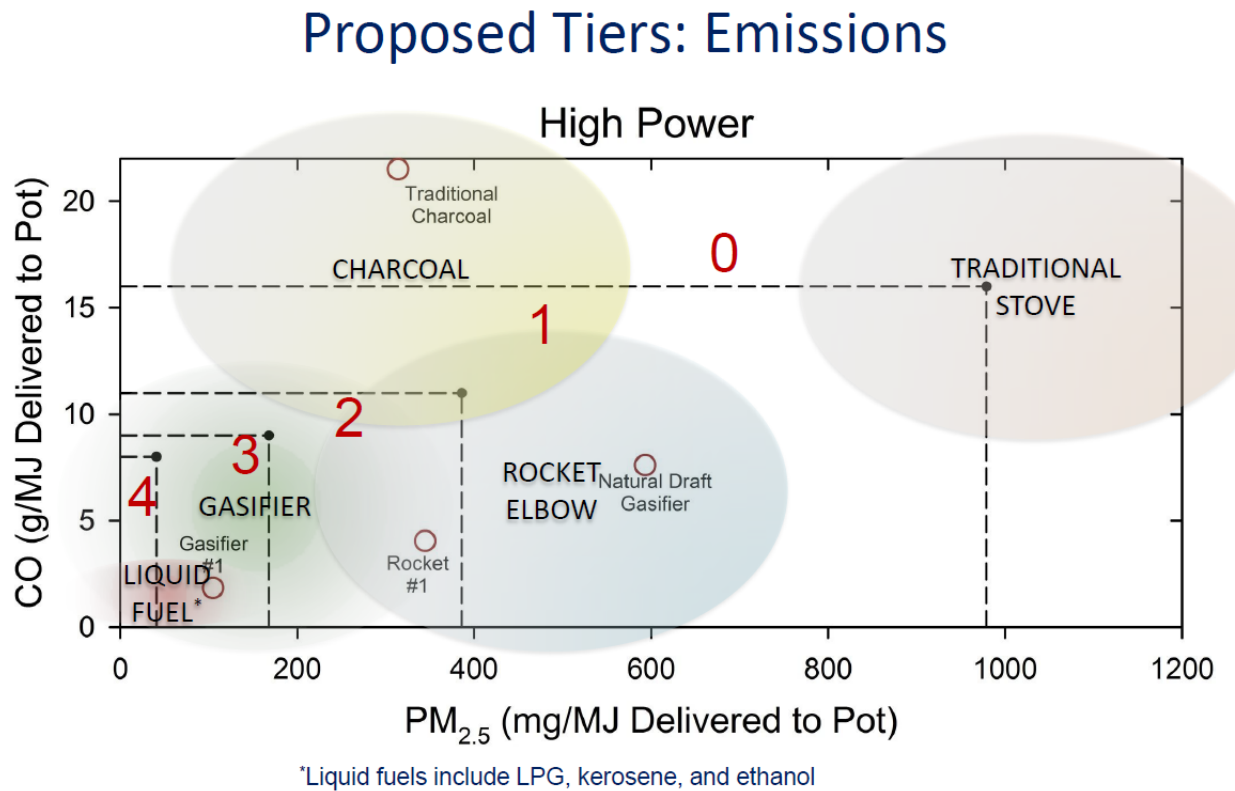
Figure 1: General Cookstove Emission Tiers

Due to these low emissions and high combustion efficiency, gasification was chosen as the combustion scheme for fecal fuel by Loveldi in his previous work on the fecal combustor [4]. In this system, the combustion of dried fecal material begins with gasification, where the feces are heated in a low oxygen environment to produce an energy rich syngas, primarily carbon monoxide and hydrogen, that can be burned further downstream in the combustor. The combustion of syngas produces a hot exhaust gas comprised mostly of air, water, and carbon dioxide, with trace amounts of carbon monoxide, inorganic compounds, and particulate matter formed during combustion. The hot exhaust gas is routed to the incoming wet fecal solids to initiate and sustain the drying process. The heat of combustion can also be harnessed through a thermoelectric generation process to produce some or all the electricity required for the entire sanitation system. Condensation heat exchangers, solar panels, or other supplemental energy conversion devices may also be added to bolster energy generation. The electricity produced must exceed that required by the sanitation system to meet the specifications set forwards by the Gates foundation.

1.3 Research Team

The cookstoves research team is based out of CSU's Powerhouse Energy Institute. The RTTC section of the cookstoves laboratory is headed by John Mizia (research advisor), and collaborators on the RTTC project include Jason Golly (fabricator), Kyle Greer (graduate student), Kelly Banta (graduate student), and multiple undergraduate researchers who helped with different aspects of the combustor's development and testing. The original combustor(s) were primarily designed and constructed by Nathan Loveldi, who was a previous graduate student on the CSU cookstoves team. The CSU team was approached by RTI as combustion experts, so our focus has been on creating a robust and efficient combustor section for the

sanitation system by using the expertise gained in the cookstove field. The lab's specific goals include burning the fecal material cleanly, minimizing gaseous and particulate emissions, and ensuring all the fecal material burns fully. The CSU team strives to burn the fecal material as efficiently as possible, producing the most usable exhaust heat (and by extension electricity) possible from the dried feces.

CHAPTER 2: COMBUSTOR THEORY

2.1 Gasification of Fecal Fuels

The combustor designed for the Gates project is a semi-gasifier. Gasification is the process of heating a fuel in a low oxidizer environment to cause a carbon rich gas to emit from the solid fuel. The gas, referred to as syngas or pyrolysis gas, can then be burned in a number of different configurations. The air introduced directly onto the solid fuel is referred to as primary air, and it allows the carbon and hydrogens in the fuel to burn a small amount, forming partial products of combustion as the species create a carbon rich gas known as syngas. To combust this syngas, another air stream is introduced further downstream from the fuel bed. This additional airflow is referred to as secondary air, and it allows the full combustion of the carbon and hydrogen products in the syngas, forming a flame region where the secondary air and syngas meet.

For most wood pyrolysis applications, the ideal primary to secondary mass flow air ratio is near 1:4. The amount of primary air in gasification scenarios should be at or below 21% to minimize emissions and maximize combustion efficiency, which makes the secondary air injection up to 84% of the stoichiometric air value (of the base fuel) to fully combust the syngas in a 1:4 air ratio gasifier [5]. Thus, the total air injection in an ideal gasifier is near 105% of the stoichiometric value, or 5% excess air. Experimentation by Wang *et al.* indicated that an ideal air injection level exists to maximize the propagation of smoldering combustion, where any less air will retard the chemical reactions, and more will reduce the reduce the reaction temperatures via dilution, slowing the combustion process [6].

2.2 Gasification Chemistry

The energy release during the gasification and combustion of fecal fuels is mainly attributed to heat release during carbon and hydrogen reacting with oxygen. During pyrolysis, the carbon and hydrogen molecules present in a biomass fuel are broken down to base and near-base states of carbon, carbon monoxide (CO) and hydrogen [7]. This means that the volatiles in syngas can combust easily and maximize heat production since large molecules, which require energy to be broken down, are much rarer in syngas than in the base fuels. The major combustion reactions of syngas are as follows in Equation 1, Equation 2, and Equation 3 [8].

Equation 1: Carbon Monoxide Formation Reaction

$$C + \frac{1}{2}O_2 \rightarrow CO \qquad (111\frac{MJ}{kmol})$$
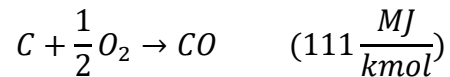
Equation 2: Carbon Monoxide Combustion Reaction

$$CO + \frac{1}{2}O_2 \rightarrow CO_2 \qquad (283\frac{MJ}{kmol})$$
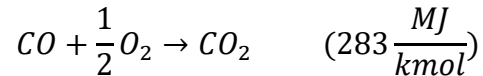
Equation 3: Hydrogen Combustion Reaction

$$H_2 + \frac{1}{2}O_2 \rightarrow H_2O \qquad (242\frac{MJ}{kmol})$$
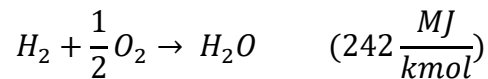
The numbers shown in parenthesis indicate chemical energy released through each reaction. The chemical reactions required to gasify biomass fuels are mostly endothermic, meaning that energy input is required for gasification to occur. However, giving the fuels enough oxygen to partially combust while gasifying will supply plenty of energy to sustain gasification without continual energy input.

CHAPTER 3: FECES AS FUEL

3.1 Comparison of Fuels

From calorimetry and ultimate analyses, seen in Table 1, the chemical composition of human feces was deemed close enough to wood biomass that setting a strict 1:4 air ratio was reasonable. The analysis for canine feces was included as well since it was used as a readily available surrogate to human feces for multiple combustor tests. Full results of the fuel analyses can be seen in Appendix D.

Table 1: Fecal Fuels Ultimate Analysis

Species, % mass	Carbon	Hydrogen	Oxygen	Sulfur	Ash	LHV (kJ/kg)
Human Feces (RTI)	48.85%	6.63%	20.88%	0.91%	14.83%	20854
Human Feces (India)	56.15%	6.04%	20.32%	0.45%	12.25%	18831
Canine Feces	36.45%	5.00%	22.99%	0.65%	28.52%	14114
Wood Pellets	47.2%	6.5%	45.4%	~0%	1.0%	20023

The values for wood pellets were taken from literature, with the lower heating value calculated from Equation 4 as follows, where W is the mass percent of water in the combustion exhaust, and λ is the latent heat of water [9].

Equation 4: LHV and HHV Relationship

$$HHV = LHV + W\lambda$$

$$\lambda = 980 \ \frac{Btu}{lb}, W = 0.21 \ \frac{kg \ H20}{kg \ exhaust}$$

From the above data, the chemical formula for both types of feces were calculated and compared to that of wood biomass. The final reduced chemical formula for human feces is: $C_1H_{1.62}O_{0.32}$. For Canine feces, the reduced formula is: $C_1H_{1.63}O_{0.32}$. Wood biomass follows the reduced molar formula of $C_1H_{1.6}O_{0.72}$. The similarity of these chemical formulae helped strengthen the assumption that a 1:4 airflow ratio would be adequate for both wood and fecal material combustion.

Another important component of fecal fuels for this application is moisture content and total mass. Per Rose *et al.*, feces have a median moisture content of 74.6%, with total fecal mass averaging 250 g per person, per day for low income countries, which equates to 38 grams of dry fecal material per person. From a disease prevention viewpoint, bacterial biomass makes up 25-54% of the organic (carbon) fraction of the feces [10].

Some consideration should also be given to the simplicity and decomposition of components, as previous research has found fecal sludge to ignite quickly when compared to other biomass fuels, due to the ease of decomposition of fecal materials and its relatively high hydrogen to carbon ratio [11]. The decomposition characteristics of fecal fuels are rather hard to track, as they are heavily influenced by individual's metabolic efficiency and caloric intake, among other factors.

3.2 Fan Driven Combustor

The operation of the combustor relies on a single exhaust fan. This fan creates a slight vacuum inside of the combustor in the range of 0.35 inches of water (87 Pa), creating a pressure differential between the combustor and ambient air that forces fresh air to be sucked into the combustor through the primary and secondary holes. To reduce energy usage by the combustor,

every part of the system had to be as airtight as possible. Any leak before the combustion zone would alter the primary to secondary air ratio, and any leak after the combustion zone would dilute the hot exhaust gas, cooling it down while requiring extra power input to the fan to make up for the loss of pressure from the leak. At flanges between combustor components, graphite gaskets were put in place and clamped down with eight sets of nuts and bolts. These graphite gaskets can withstand the high temperatures of combustion while retaining a seal. In lower temperature zones, silicone gaskets created a similar seal with less force required to close and maintain an airtight seal between components.

3.3 Ash Formation

The main difference between wood biomass and fecal material in terms of combustion is the amount of ash present. Wood pellets have very low ash levels, and tend to produce a fine dust-like ash that will readily fall through a fuel grate. Canine and human fecal pellets/flakes tend to form a much harder ash that retains the original shape of the fuel. This is what necessitated the original fuel grinder designs. For the ash removal to be effective, excess ash had to be occasionally eliminated without disturbing the pyrolyzing fuel or the combustion zone. It also had to survive in the high temperature environments near the fuel grate, where ash was formed. Multiple ash grinder blade and shaft configurations were tested to find an effective and robust ash removal solution. The final ash blade was made from 1/8" stainless steel plate, cut then welded into a flat blade topped with a V shape to allow some extra fuel mixing, seen below in Figure 2 and Figure 3. The shaft of the grinder was widened multiple times over the different models to prevent any bending or warping in the high heat environments. The final grinder shaft was a tube that had a small hole drilled at its base to allow a set screw to fully lock the shaft into place.

Figure 2: Ash Grinder Blade and Shaft

Figure 3: Ash grinder blade inside of combustor

To allow for ash collection and removal, an ash cup was added below the fuel grate. This ash cup has a silicone gasket since it is well below the combustion zone and therefore does not require the high temperature graphite gasket to maintain a seal. The ash cup is connected to the combustor by a detachable hinge and latch. This setup allows for easy ash disposal between combustor burns. The ash cup size can be easily modified for different applications since the most important aspect of the ash cup, the silicone seal, is independent of reservoir size. To keep up with ash formation, the ash grinder is run for one to two seconds after each fuel addition. This timing allows ash to be removed from just on top of the fuel grate without removing the unburnt fuel higher up above the fuel bed.

CHAPTER 4: COMBUSTOR HISTORY

4.1 Previous Combustors

The fecal combustor has gone through multiple iterations to reach the current version,

denoted as the Beta combustor in this document. The original combustor designs were based on

a downdraft combustion mechanism, and multiple combustion chambers and related

modifications were designed and tested by Nathan Loveldi [4]. Downdraft combustors have the

advantage of flowing pyrolysis gas through a hot char bed before the syngas is ignited, so the

char bed acts as a source of preheating for the air/syngas mixture. The most advanced downdraft

version of the combustor included multiple features that reduced particulate emissions and

improved reliability. An ash grinding blade was inserted through the main fuel grate to remove

burnt out ash, which is insignificant for wood fuels but much more problematic in fecal

materials. Carburetors for primary and secondary air inlets were added to allow modulation of

airflow ratios as the final system runs with a fan pulling air through the combustor as opposed to

mass flow controlled air being forced in. A hot air igniter allowed the ignition element to be

removed from the harshest combustor environments near the fuel grate, where ignition coils were

initially used. A catalogue of the different combustors can be found in Appendix E.

4.2 Downdraft Combustor

In the downdraft combustor, the secondary air inlet was sheathed so that the air flowed

over hot steel around the combustion zone before being rerouted to the secondary air holes at the

flame. This preheating of secondary air helped to increase combustion efficiency and reduce

particulate emissions by cooling pyrolysis gasses less before combustion. When switching from

forced air to fan pulled draft, the excess sheathing proved too much pressure drop for the fan to

overcome to maintain proper airflow rates through the combustor. In addition, the high thermal mass of the downdraft combustor caused the heat up time to a steady state temperature to be prolonged. Insulation on the combustor exacerbated this problem and a true steady state in this combustor became difficult to determine. A detailed summary of batch-fed downdraft combustor experiments conducted by Cranfield University, who purchased a v1 downdraft combustor via reinvent the toilet challenge collaboration, showed modified combustion efficiencies between 67 and 80 percent in the downdraft v1 combustor [12]. Results from more recent combustors can be seen for comparison in Section 10.4. An important phenomena, witnessed during batch-fed combustion, was that the smoldering that leads to pyrolysis gas release is mainly a function of oxidizer and fuel availability [13]. When large amounts of fuel and oxidizer are available, the system can easily enter a state of thermal runaway where heat release is excessive and nearly uncontrollable. Figure 4 and Figure 5 below show the downdraft combustor, and a downdraft combustion scheme.
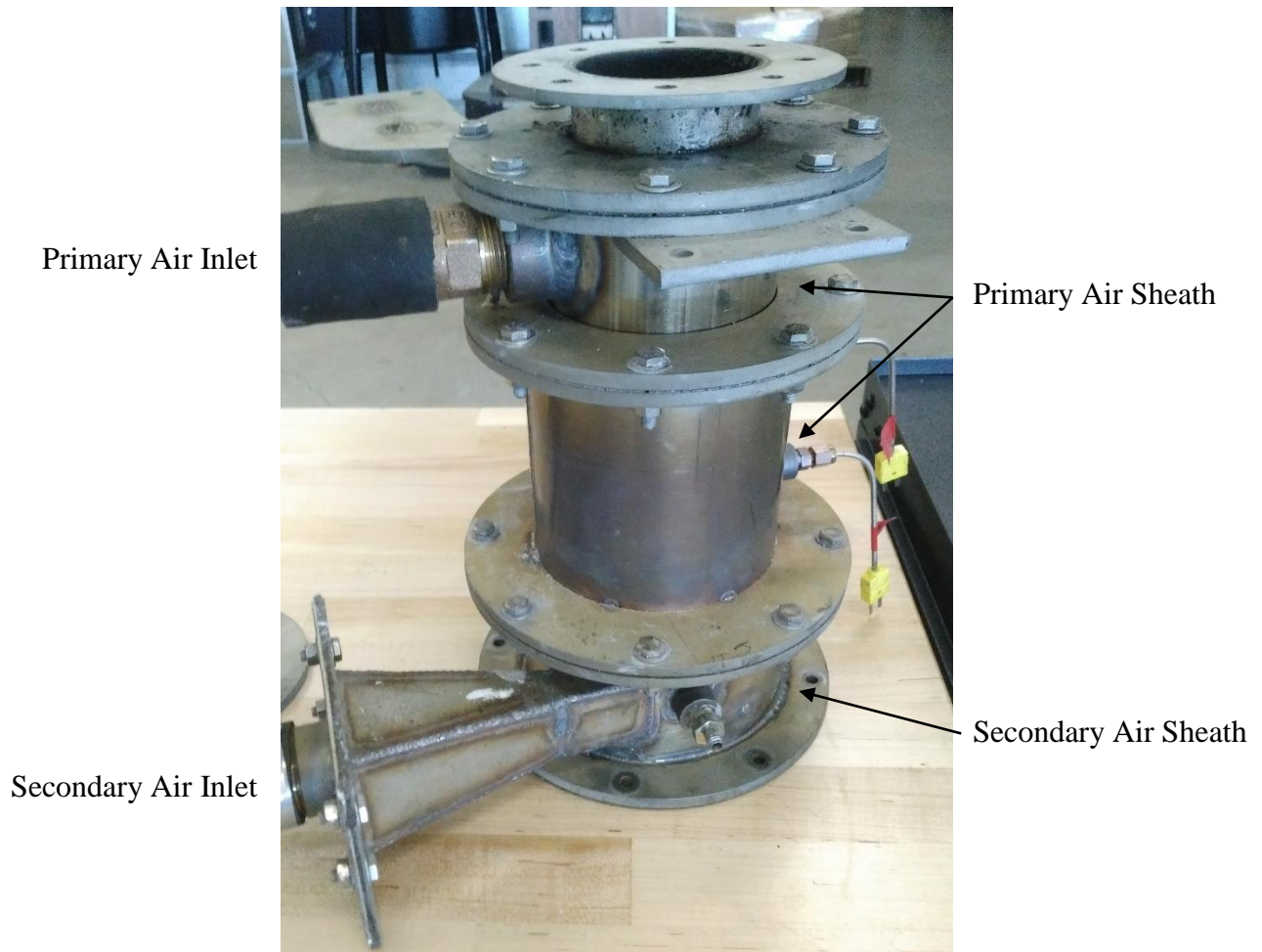
Figure 4: Downdraft V1 Fecal Combustor
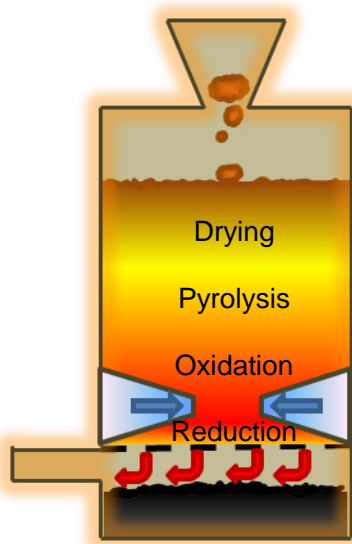
Figure 5: Downdraft Gasification Schematic

4.3 Micro Combustor

A less thermally and physically massive combustor was constructed to try and simplify the original downdraft combustor. While the original downdraft combustor was 29kg, the micro combustor weighed only 3kg, with the reduced material weight leading to a lower thermal mass as well. It had a single tube inlet for primary air, and a single row of uniform holes for secondary air. The secondary holes were sheathed by a single inlet manifold to equalize pressure and flowrate through each secondary air hole. Downdraft combustion of syngas proved difficult in this combustor. Downdraft combustion also required an "airlock" between the fuel inlet and fuel grate, to prevent hot syngas from flowing up through the unburnt fuel storage as opposed to down through the grate and to the combustion zone. As a side experiment the combustor was flipped upside down and run in an updraft configuration to see if the same types of emissions could be achieved without the need for an airlock. The updraft gasification process proved to be simpler to control, similarly efficient to the original downdraft combustor, and much more stable in terms of flame position/heat production. Figure 6 and Figure 7 below show the micro combustor (situated for updraft combustion), and an updraft combustion scheme.

Figure 6: Micro Fecal Combustor, Updraft Position
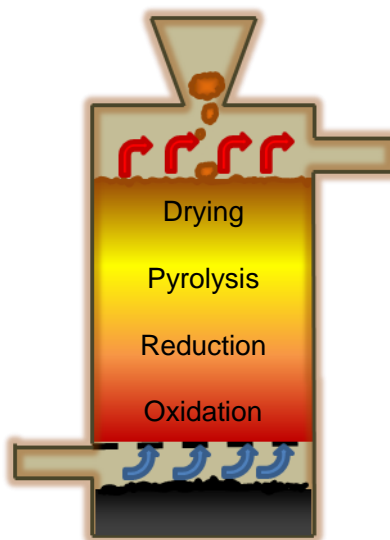
Figure 7: Updraft Gasifier Schematic

4.4 V2 and V3 Micro Combustors

The main perceived issue with the "flipped" micro updraft combustor was lack of primary air mixing. To address this issue, a second version of the micro combustor was constructed with identical primary and secondary inlet holes. The hole geometries on this micro combustor v2 were not sized for any specific airflow ratios since it was controlled by forced (mass controlled) air. To once again transition to a fan-driven system, the micro combustor v3 was built. This combustor had primary and secondary air injection holes specifically sized to create a 4:1 airflow ratio when both primary and secondary inlets were held at the same pressure. Aside from hole inlet size, the v3 combustor is identical to the v2 combustor. The v3 combustor can be seen below in Figure 8.
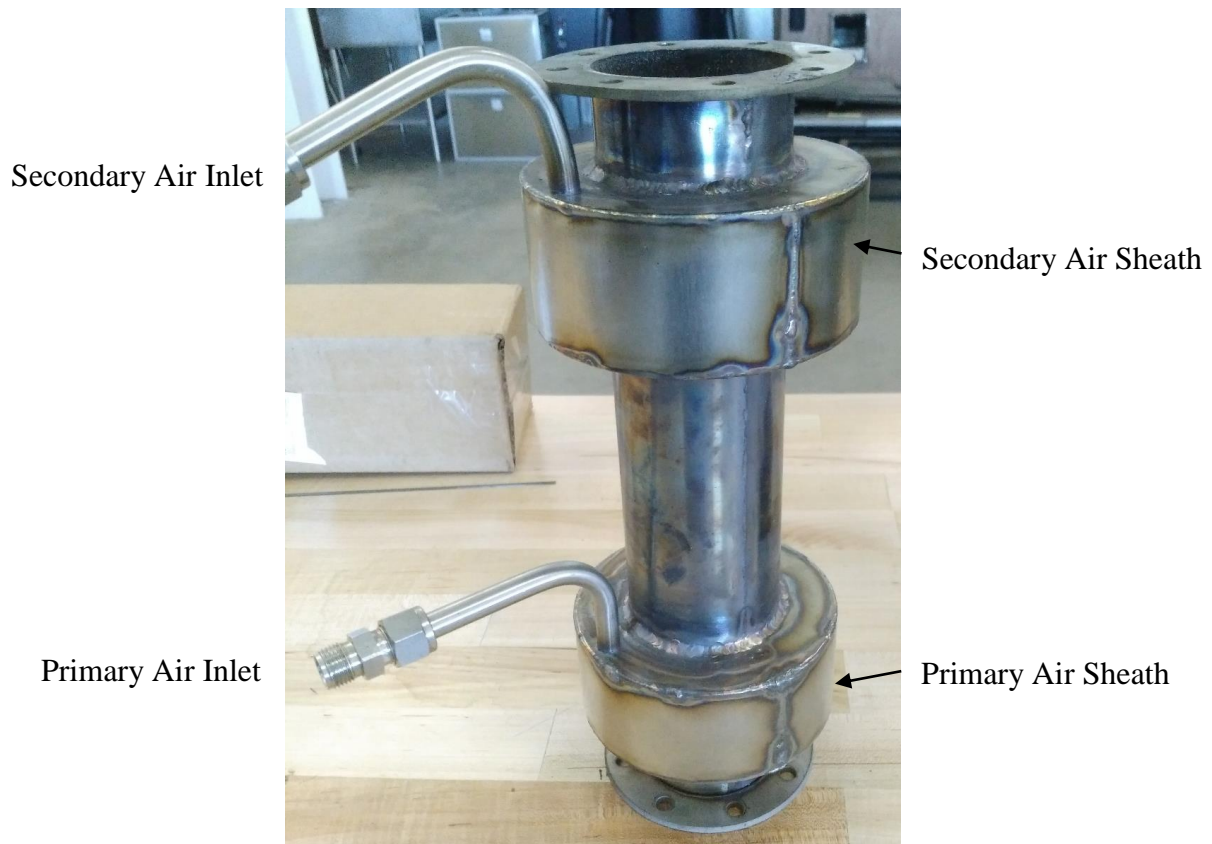
Figure 8: V3 Fecal Combustor

A comparison of emissions between the v2 and v3 combustor can be seen in Figure 9. The carbon monoxide emissions from the V3 combustor are lower during steady state emissions, and when averaged the total carbon monoxide emission from the V3 combustor was lower than those from the V2 combustor. Since the only change between the v2 and v3 combustors was hole geometry, the improved CO emissions from the v3 combustor most likely stem from the lower air injection velocities introduced through the slightly larger secondary air holes.
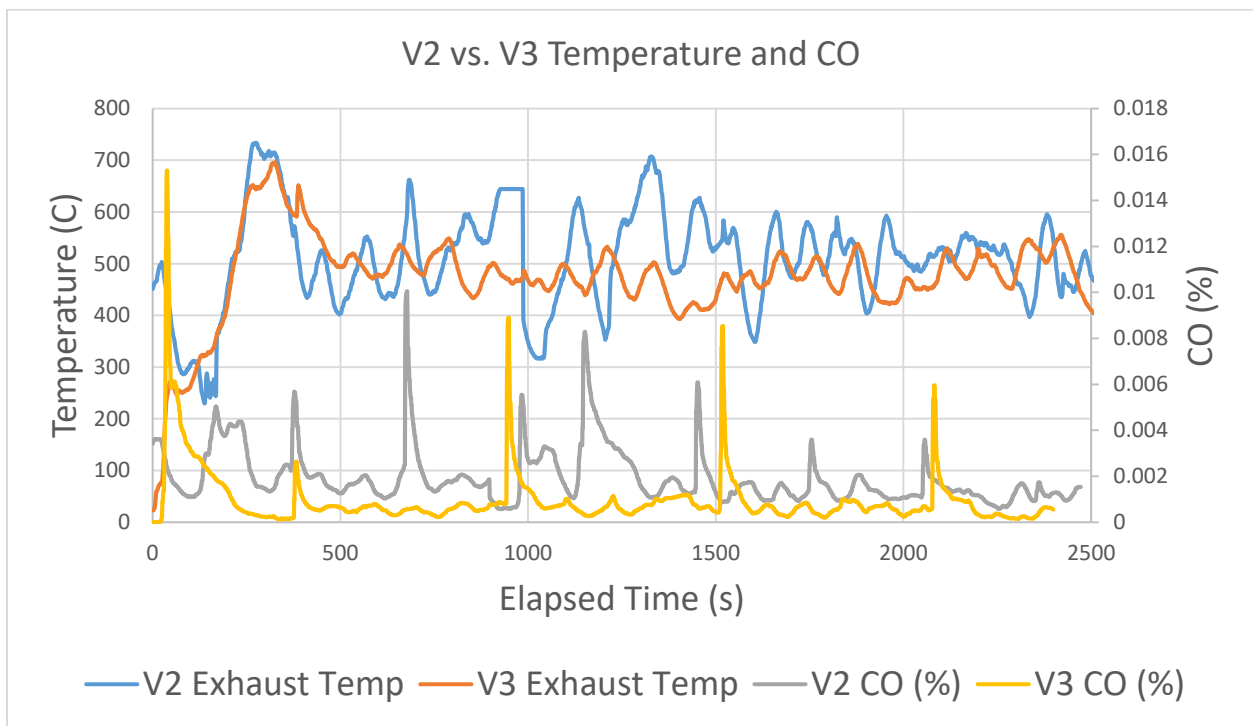
Figure 9: V2 vs. V3 CO Emissions

The micro combustor v3 proved itself to be a very stable and reliable combustor when burnt with wood pellets. In a forced air configuration, the v3 combustor achieved 24-hour wood pellet burns without incident. Multiple different approaches for ash removal were tested with the micro combustors, but once again ash grinding proved to be the simplest and most robust process available. The micro v3 combustor was the first to operate reliably when fully integrated with

ash grinder, fuel auger, air igniter, exhaust stack and exhaust fan. Because of its small forced air inlets, the micro v3 was not well designed to work when controlled by the exhaust fan alone. To move to a fully fan-driven system, a new type of air inlet for the micro combustor was necessary.

4.5 Monofold Combustor

The new fan-friendly design was constructed with a single manifold sheathing both the primary and secondary air inlet holes, earning it the name "monofold" combustor. This single manifold ensured that the inlet pressures for primary and secondary air were equal. To evaluate the pressure inside of the combustor, an inlet was created through the manifold directly into the combustion chamber, halfway between the primary and secondary inlet holes. Another hole into the combustion chamber was necessary for the air igniter to have direct access to the fuel bed. To operate reliably, the combustor needed to always have airflow entering either from the air igniter or the inlet manifold. A levered door system was created to ensure that both inlets could not be closed at the same time. Once the igniter, ash grinder, fuel hopper, exhaust fan and pressure transducer were all fixed to the v3 combustor, it was prepared to be the first fully hands-off, fan driven combustor system. When the combustor's automation code was started and the fuel hopper filled, the combustor could run for an indefinite amount of time without any manual inputs. A schematic of the monofold with labeled inlets and ports can be seen in Figure 10.
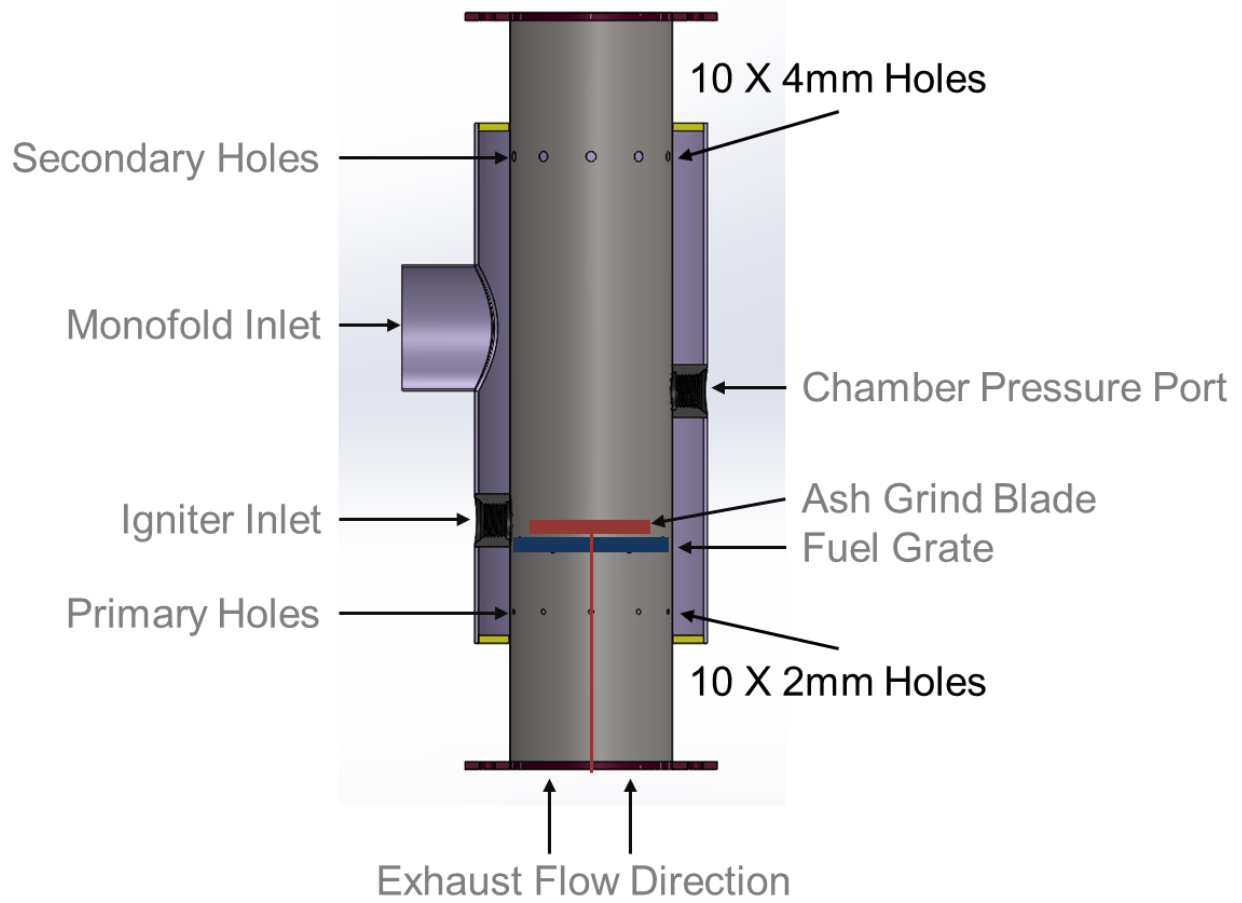
Figure 10: Micro Monofold Schematic

5.1 Combustor Body

The majority of mechanical and electrical components for the combustor have been replaced or improved multiple times over the life of the project. The combustor body is created by water jetting stainless steel with the combustor shape and air injection holes. The combustor body must be rolled into shape and then welded in place. The air sheath (monofold), fuel grate, and other combustor sections are also formed from water-jetted steel. Separate sections of the combustor are connected via eight hole flanges with a graphite gasket in between. Below the combustor is another custom-built section containing a hinged ash cup for easy ash removal. The section above the combustor has a slanted slide into the combustor where the auger is attached. The stainless steel and graphite construction ensures that the combustor has high heat tolerance and enough longevity to be feasible in a sanitation environment. The combustor body can be seen in Figure 11.

Figure 11: Monofold Combustor Body

5.2 Ash Grinder

The ash grinder blades are made from stainless steel blades on a long section of stainless pipe. That pipe is routed through the fuel grate and out the bottom of the combustor where it connects to the ash grinder motor via a small coupler. The interface where the ash grinder shaft exits the combustor is sealed with a welded-on boss and Swagelok fittings. This Swagelok fitting interface is filled with a small amount of sealant material to ensure minimal air leaks through the ash grinder shaft. The interface can be seen below in Figure 12.

Figure 12: Ash Grinder Interface

5.3 Monofold Flapper

The monofold flapper device uses water-jetted clamps and fixtures that come together to form two doors, one for the monofold and one for the igniter. These doors are finished with a high temperature silicone pad to allow for sealing on each opening's surface. Linkages to a Firgelli L12 linear actuator are located on each door. To keep the igniter open during ignition sequences, a small spring pulls back on the igniter door. To allow the igniter to close during steady state, a stopper is placed behind the monofold door, which will force the mechanical action of the actuator to close the igniter door as opposed to further opening the monofold door. The flapper device can be seen below in Figure 13. The Firgelli linear actuator used in the monofold flapper device is actuated via a simple 1-5V input signal, and powered by a low-current 5V source. The control signal for the actuator is created by a NI analog voltage output module.

Figure 13: Monofold Flapper Device

5.4 Exhaust Fan

The exhaust fan used to run the combustor has changed multiple times, though any fan in the proper voltage range with enough airflow could theoretically be used. The fan runs between 6V and 18V during normal combustor operation, depending on the pressure differential needed by the combustor. The fan has been powered by two separate methods. The first (mainly experimental) method involves sending a 0-10V signal from a national instruments (NI) analog output module to a voltage doubling circuit (simple op-amp circuit) then through a linear voltage regulator fed with 24V power. The voltage regulator amplifies the current of the doubled signal, allowing it to run the fan. The second (and likely final) fan control involves a pulse width modulation (PWM) motor regulation chip which receives an input signal between 0-5V and outputs a signal (amplified by a power source) that is capable of running the fan. The auger and grinder motors need only be timed for proper fuel addition/ash removal to be used with the system. Both the auger and grinder motors are fed their power through a relay, which is actuated via a NI digital output module.

5.5 Hot Air Igniter

The heat required for ignition is achieved with a Rauschert 110V hot air igniter, which is also controlled via relay/digital signal. This igniter contains a highly efficient heating element cased in a ceramic shell that effectively heats any air flowing over or through it. An image of the igniter can be seen below in Figure 14 [14]. A heat versus airflow graph can be seen in Figure 15. The igniter is encased in a stainless piece of tubing that has been machined to hold the igniter in place near the fuel grate. The tubing is welded to a small threaded section that screws into a boss on the combustor body directly above the fuel grate. The back side of the igniter body is flat for sealing purposes.

Figure 14: Hot Air Igniter
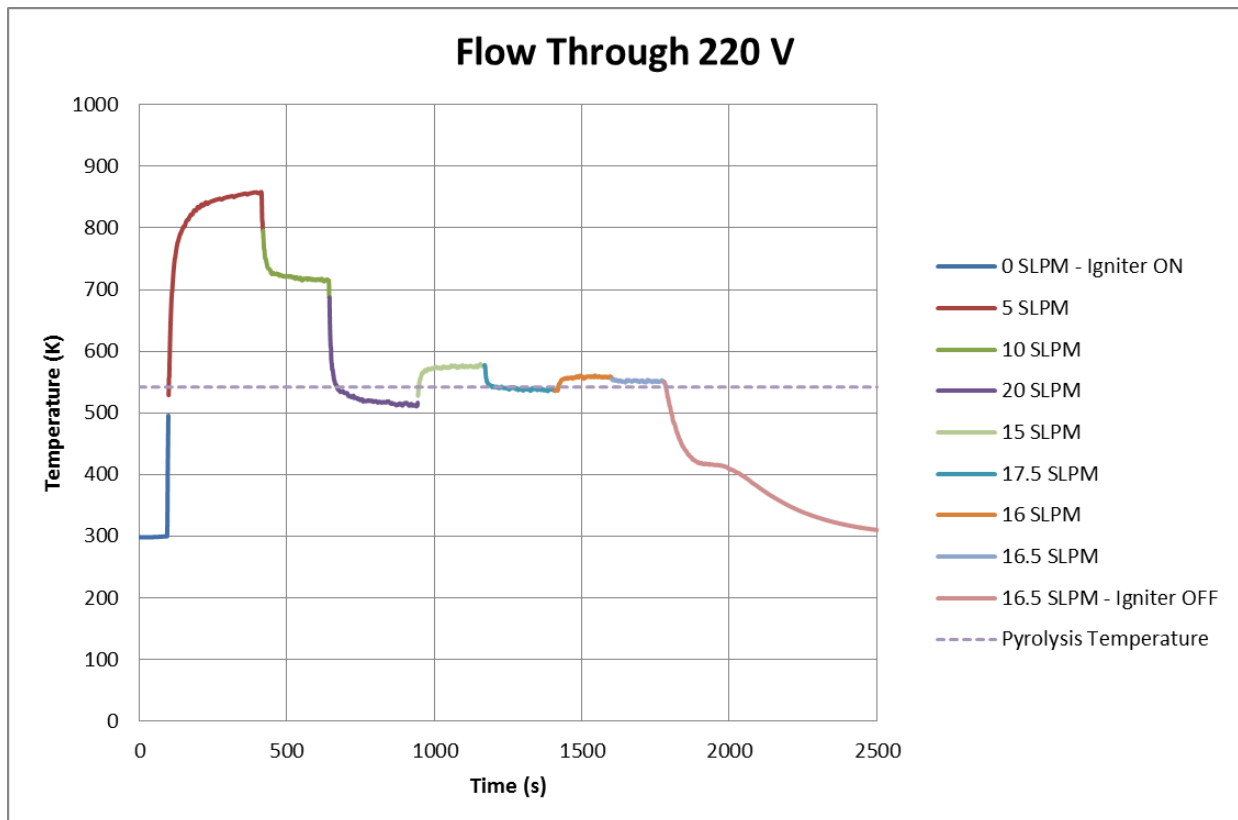
Figure 15: Igniter Temperatures at Different Flows

5.6 Pressure Monitoring

A zero to one inch of water pressure transducer interprets the pressure inside of the chamber in relation to ambient pressure. The measurement is taken from inside the combustion chamber, between the primary and secondary air inlets. A boss (similar to the igniter boss) is welded through the monofold and into the combustion chamber. A short section of stainless tubing is connected to the boss, and that metal tubing connects to a flexible rubber hose. The hose is routed up to the pressure transducer where it is connected to the low pressure inlet, with the high pressure inlet open to ambient air. The small section of steel tubing helps ensure the flexible tubing will not melt. The transducer itself produces a 0-5V signal based on the pressure differential it sees. This signal is fed into a NI analog input module, which allows us to calculate the pressure based on the transducer signal.

5.7 Temperature Monitoring

A fourth NI module is dedicated to thermocouple measurement. The experimental combustor system tracks temperature in multiple places, including: near the flame zone, in the exhaust path, and past the exhaust fan. The four NI modules (digital output, analog input, analog output, thermocouples) form the basis of the combustor control scheme. The input signals for the control scheme are the combustor pressure and the temperature nearest the fuel bed. The outputs include control signals for all the components listed above. A model of the fecal combustor with all its current modifications can be seen in Figure 16.
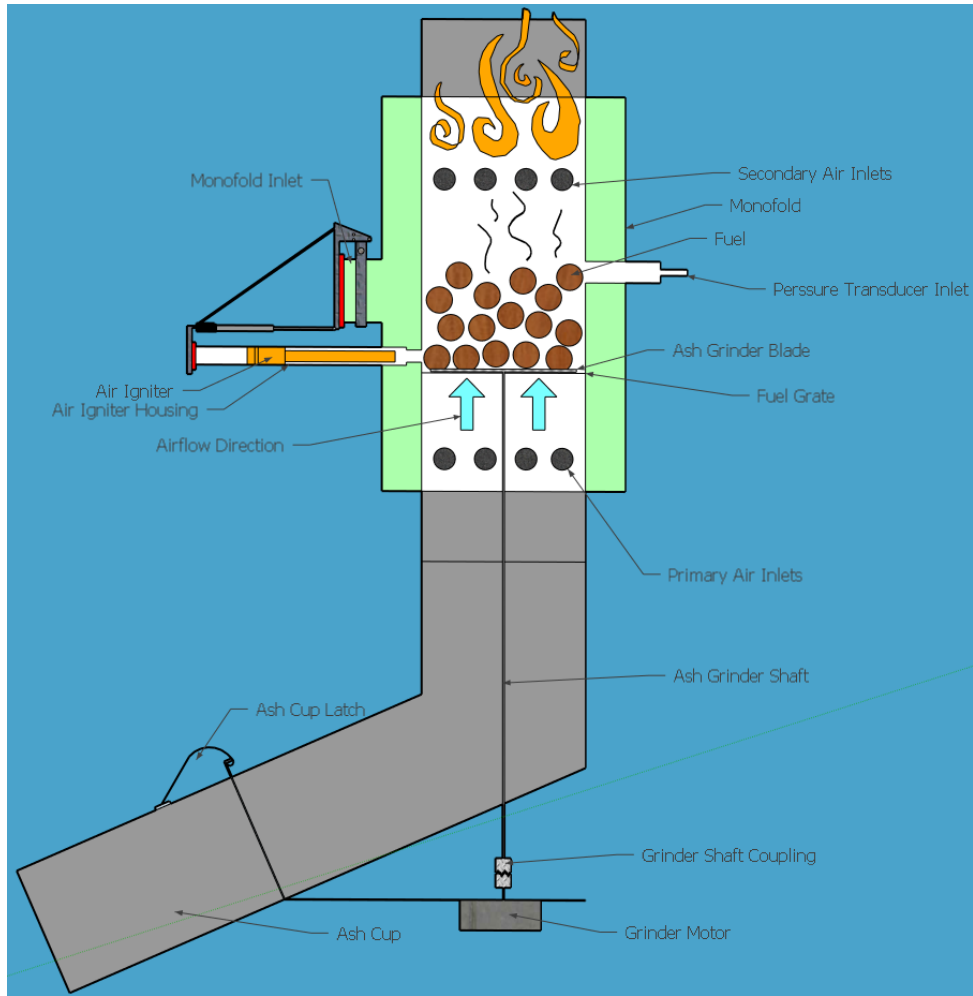
Figure 16: Monofold with Combustion Hardware

CHAPTER 6: FUEL ADDITION TECHNIQUES

6.1 Fuel Feed Performance Metrics

Multiple methods of fuel addition have been tested throughout the combustor's development. The main criteria for fuel addition into the combustor are fuel drop size, fuel feed rate, and power consumption. Fuel drop size refers to the amount of fuel added during one "addition". For continually feeding auger systems, the fuel drop size is measured as grams of fuel dropped into the combustor per second as opposed to grams per addition. Fuel feed rate is a measure of how quickly or slowly the fuel additions occur. The high end of feed rate, where fuel is added as fast as possible, often set a limit on how high the firepower in the combustor could get. The low end of feed fuel rate was primarily important for keeping higher energy content fuels burning well. If a fuel addition method drops fuel loads that are too large or too frequent, it can destabilize the flame and increase harmful emissions. Energy consumption from fuel additions is rather straightforward, and is measured as the amount of electrical energy consumed by the fuel feed motors per gram of fuel added to the combustor. Energy consumption is a concern for the final system, but was given a low priority for the prototype system to make combustor stability and emission the primary focus.

6.2 Original Lidded Hopper

The original fuel addition method at CSU was a short stemmed (~1ft) auger that fed from a hopper into the combustion chamber. As there was no fuel drying system in place at CSU, a sealed lid was added to the top of the hopper to reduce pressure losses through the fuel/auger during normal operation. The hopper was sized to be able to burn for at least a few hours before any refueling was necessary. Because of the sealed hopper lid and the rest of the exhaust

pathway on the CSU system, the pressure and airflow inside of the system was very easy to control with the exhaust fan and the fan was normally operating around half of its designed power draw. The feed rate was perfectly adequate to achieve any firepower the fan/combustor system could handle, but the fuel dropped in bursts that were much larger than expected as opposed to a consistent, controlled addition of fuel. These large drops occurred whenever the end of the auger blade was rotating near the bottom of the auger shaft, whereas very little fuel was added whenever the auger blade was rotating near the top of its shaft. The large fuel additions were much more likely to extinguish the flame whenever too much unburnt fuel dropped through the combustion zone at once, destabilizing the airflow and flame front. A picture of the lidded hopper can be seen below in Figure 17.
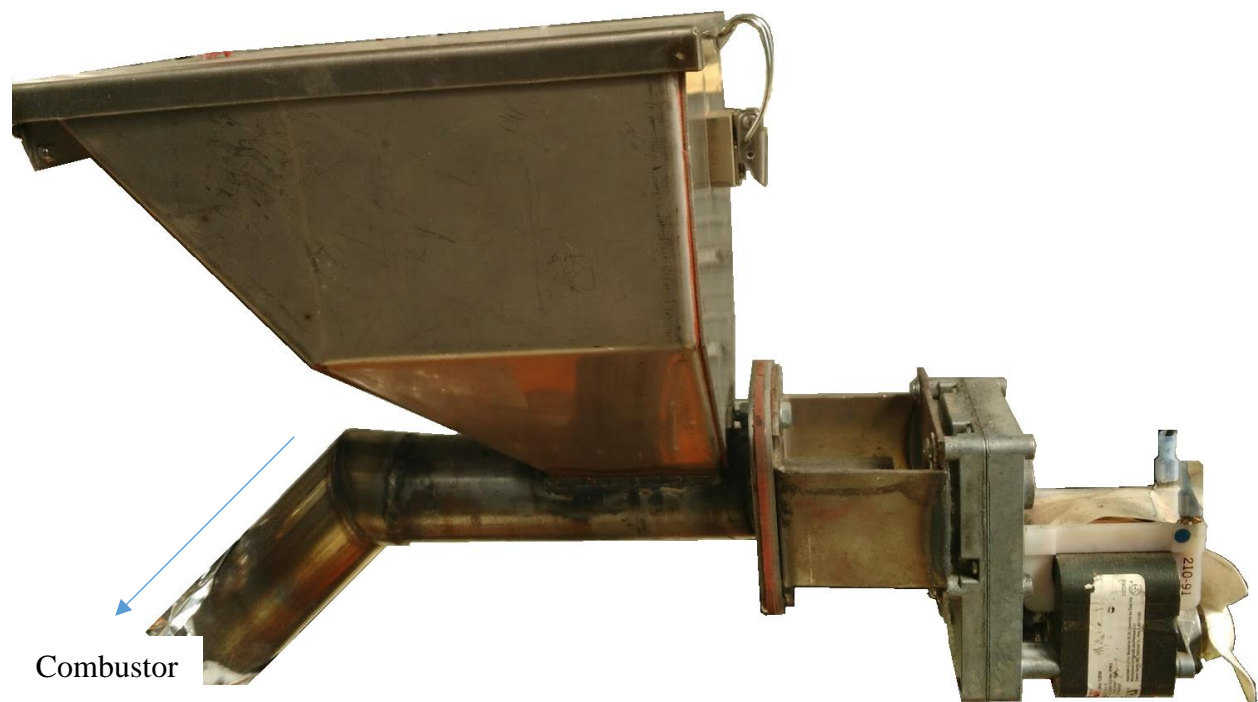
Figure 17: Lidded Hopper and Auger System

6.3 Long Shafted Auger

As the fecal drying system progressed, the need arose for a fuel hopper that was further away from and lower down than the combustor. These criteria were meant to accommodate a "tumble dryer" for semi-dry feces to pass through and then drop into the fuel feed system. The size and leaks of the tumble dryer ended up being problematic, and the dryer was eventually replaced with a drying plate system that could be located directly on top of the combustor, with a much closer fuel hopper. To meet the tumble dryer requirements, a much longer shafted auger (approximately three feet long) was put in place of the old auger, and it was placed on a slant so that the fuel hopper sat much closer to the ground. The fuel hopper was kept open in this case, so that the fuel being dried could drop right into it. Since the hopper was open, air was allowed to leak through the auger shaft and into the combustor. Luckily, the long auger shaft would fill with enough fuel that the pressure loss inside the chamber was minimal. The long auger ran on a much slower motor than the previous auger system, which meant that the fuel feed rate was much lower in general. The long auger had a smaller shaft, and the fuel drop-in point was located a few inches before the end of the auger blade. Both factors helped to reduce the fuel drop size from the auger, as well as helped even out the rate of fuel addition. The low feed rate ended up hindering ignitions, where insufficient fuel entered the combustion chamber during the 60 seconds of igniter pre-heating. The feed rate also limited the maximum firepower of the combustor for fecal fuels, but had little effect on the ability to burn wood pellets as their energy density is so much higher. The long shafted auger can be seen below in Figure 18.

Fuel Chute,
Combustor

Figure 18: Long Shafted Auger with Hopper

6.4 Fuel Feed Piston

The third feed rate system was built to work with the plate dryer system and was

designed to reduce variability in fuel feed rate/fuel drop size, as well as alleviate some of the

pressure loss issues that come from an open fuel hopper. A hopper, placed directly under the drying plate to catch freshly dried fuels, was installed above a small piston cylinder. The piston cylinder extended past the hopper to connect the fuel feeding mechanism to the fuel chute, which allows fuel to slide into the combustor without disrupting the exhaust path. A piston was located inside of the small cylinder to push a set amount of fuel into the chamber at a time. The piston was operated via a linear actuator which could be ran either forwards or backwards to move the piston. The piston head sealed the chamber off from the fuel hopper whenever it was in its forward most position. Whenever the piston moved backwards, fuel from the hopper would drop down into the piston cylinder where it could be pushed into the combustion chamber upon the next piston cycle. When the piston was anywhere but its forward most position, a rather large air leak was created that reduced the differential pressure in the combustor. The leak created was frequently in excess of 0.1 inches of water, which is nearly a third of the designed pressure differential in the combustor during steady state (0.35 inches of water). The large leak created would change the flame and exhaust dynamics in the chamber, and make it more difficult to have consistent steady state temperatures at the drying plate and further downstream. The main advantage of the piston system was fuel drop size, since it was consistent and not large enough to disrupt the flame inside of the chamber. The fuel drop rate, however, was limited by the amount of time it took to move the piston fully back and forwards again. Some of the less dehydrated, lower energy content fuels were not able to sustain a flame even at the maximum feed rate, and would instead extinguish between fuel addition and relight whenever more fuel dropped in. With the lower energy content fuels, power consumption of the piston system was similar to that of the auger systems since the linear actuator was always in motion. For wood pellets and other high-energy content fuels, the power consumption was considerably lower since the piston could

sit inactive between fuel additions. However, the faster (first used) auger system had the same advantage of being able to wait between fuel additions without the negatives of wild pressure fluctuations and low feed rate. The fuel feed piston can be seen below in Figure 19.

Fuel Chute,
Combustor
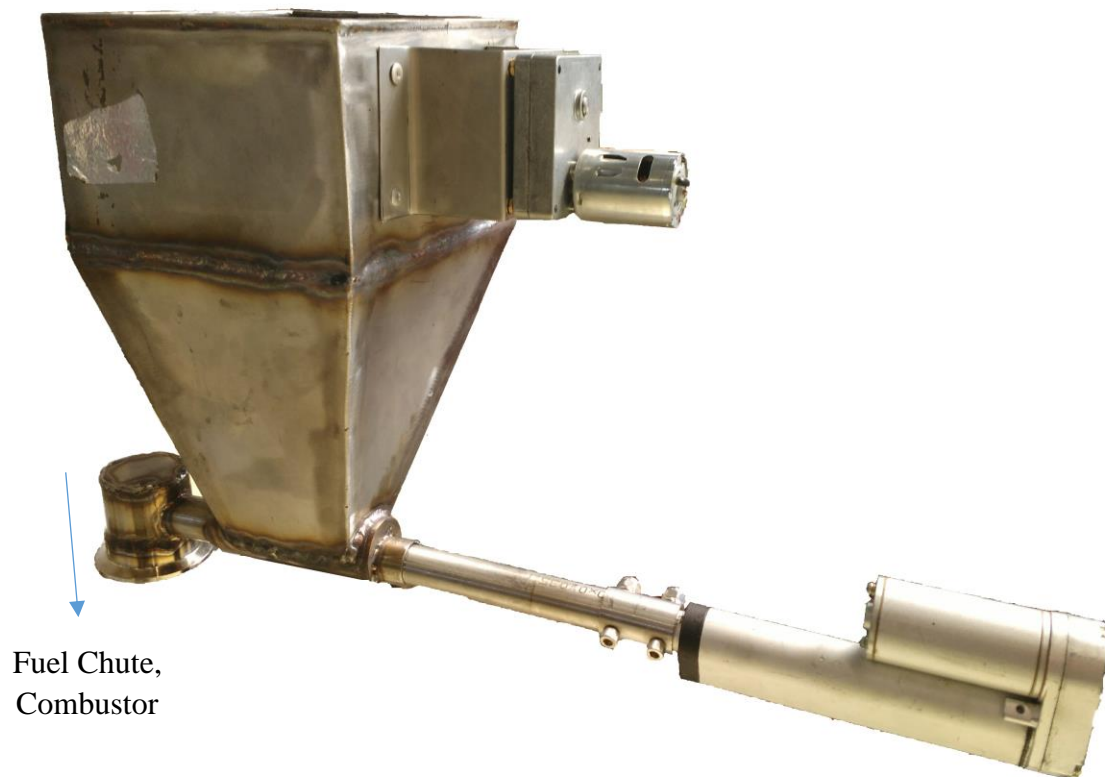
Figure 19: Fuel Feed Piston with Hopper

6.5 Fuel Feed Comparison

A comparison of the three major fuel addition systems can be seen below in Table 2. For each system, fuel feed rate was found gravimetrically by removing the fuel feed tube from the combustor and instead directing it towards a logging scale. When measuring flow rates of feces, fuel bridging was often a problem just above where the fuel drops in to the auger/piston cylinder.

To combat this, the fuel in the hopper was either kept low enough to not bridge, or was manually moved into the fuel feed cylinder. Future designs of the fuel hopper will be designed to minimize any bridging and ensure consistent fuel additions.

Table 2: Feedrate Systems Comparison

Fuel Feed System	Short Lidded Auger	Long Auger	Piston
Max Feedrate (g/s)	1.05	0.2	0.22
Minimum Fuel Drop size (g)	1.05	0.2	3
Maximum Firepower (kW)	21.9	4.2	3.6
Pressure Loss	Minimal when lid is closed	Moderate with fuel in auger	Severe when open, minimal when closed
Power Consumption (W/g, approximate)	2.3	12	14.1

The above values for firepower were calculated from the lower heating value of dehydrated human feces from RTI multiplied by the maximum feederate of the different fuel feed systems. The firepowers shown could only be achieved at 100% modified combustion efficiency. Maximum firepower for each feed system was calculated as shown in Equation 5.

Equation 5: Firepower Approximation

$$Firepower\ (kW) = Feedrate\ \left(\frac{kg}{s}\right) * Lower\ Heating\ Value\ \left(\frac{kJ}{kg}\right)$$

CHAPTER 7: COMBUSTOR CONTROL SYSTEM

7.1 Controls Overview

Onabanjo *et al*. found that even in optimum gasification conditions, systems designed to run off of fecal fuels will need to "operate on fuels with varying fuel characteristics, in particular moisture and ash contents, and adapt operation to the varying fuel processed from the toilet units to maintain its performance" [15]. In an effort to maintain consistent and efficient burns, a combustor control system was designed using LabVIEW to interface with the various combustor components. The electronic components controlled using LabVIEW include the exhaust fan, fuel auger motor, linear actuator to control the monofold flapper, hot air igniter, and ash grinder motor. The software also reads in the temperature from thermocouples and differential pressure from the transducer that reads the pressure in the middle of the monofold combustor. The decision making in the code relies on the thermocouple closest to the fuel bed and the pressure measurement inside of the combustor. The general control flow can be seen on the following page in Figure 20.
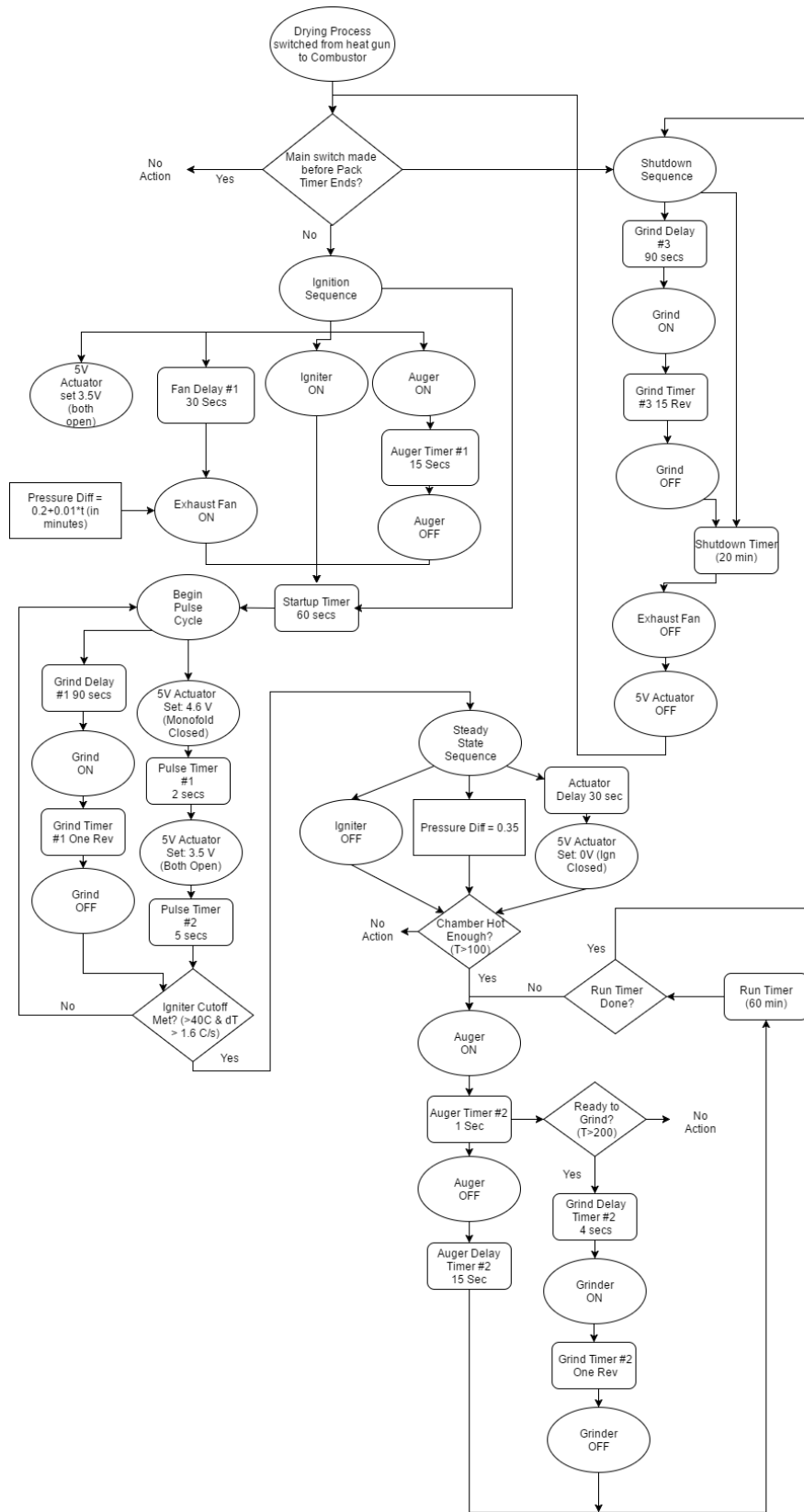
Figure 20: Combustor Control Flow Diagram

7.2 Ignition Sequence

The ignition sequence begins any normal burn. At the beginning of ignition, the exhaust fan is off and both the monofold and igniter flapper doors are open. To begin ignition, the igniter is turned on and the auger is activated for a set amount of time to allow a starting charge of fuel into the combustor. The pressure setpoint for the fan to reach is set to 0.2 inches of water, and increases by 0.01 inches of water every minute. A standard PI controller with gain of 8 and integral time constant of 0.03 is utilized to create the fan voltage signal. This controller is operated on a one second time basis, due to the slower read rates of the thermocouples and pressure transducer that dictate the fan's setpoints. Once one minute has elapsed, the flapping action begins on the monofold. The monofold door closes most of the way, forcing more air to travel through the igniter. After two seconds, the monofold door returns to its' open position for five seconds. This cycle repeats until ignition occurs.

While the ignition sequence is active, the pressure setpoint for the fan to maintain continually increases to keep pace with the higher amounts of syngas that are produced as the hot igniter air reaches more of the fuel bed. Ignition is detected as a change in the temperature near the fuel bed. The change in temperature per second is averaged over four seconds, and once that value has exceeded 2.0 degrees Celsius per second, the controls assume ignition has occurred. A pressure spike also indicates ignition, but it is often too quick of an event to be relied upon by the control scheme.

7.3 Steady State

Once ignition is detected, the ignition sequence ends and the steady state control sequence begins.   This begins with the monofold flapping ending, while the exhaust pressure setpoint changes to 0.35 inches of water. Once 30 seconds have elapsed, the linear actuator fully

extends, causing the monofold door to fully open and the igniter door to fully close. The 30 second wait to close the igniter door allows a more fully developed flame to occur before changing airflow regimes. Otherwise the flame would be focused next to the igniter hole and might not be able to withstand the airflow transition. The auger does not turn on immediately after ignition, but instead waits for a higher temperature near the fuel bed. This temperature is typically 65°C, and it ensures that the flame region will be robust enough to survive solid fuel falling through it and disturbing the pyrolysis zone.

Once this temperature is reached, fuel additions begin in timed intervals, where the auger is turned on for a set amount of time (1 second) then off for a period between fuel additions (15 seconds). The on and off times for the auger are part of what dictate firepower of the combustor, and they must be changed for different types of fuels to prevent the flame from extinguishing or the fuel zone from growing too much. Fuel addition timing controls a large portion of the combustor emissions, as well. Less frequent fuel additions will help the combustor achieve more steady flames and have less periods of transience, where flame instability leads to low combustion efficiency, higher carbon monoxide levels, and worse particulate emissions. However, less frequent additions require larger additions, which also negatively affect the combustor performance by disturbing the fuel bed and creating more smoke before a larger flame can develop to accommodate the larger amount of syngas.

There is one more temperature criteria inside of the steady state sequence, and it dictates when grinding can occur. Once the combustion chamber reaches 300 °C, the grinder turns on once per fuel cycle. Grinding below this temperature would run the risk of disrupting the pyrolysis zone and extinguishing the flame. Waiting too long to grind would create the possibility of a large ash buildup that would hinder pyrolysis and flame stability. The grind

controller includes wait and grind time settings. Wait dictates how many seconds after the fuel addition the grinder must wait from the beginning of the fuel addition before activating. The grind time sets how long to grind for, again differing based on the fuel used. For human feces, the grind wait is set to four seconds post fuel addition, and the grind time is set to three seconds. The grind time has to be relatively high (three seconds per fifteen second fuel cycle) for fecal fuels because of their high ash content. For wood pellets, grinding is unnecessary as wood ash falls through the fuel grate without being ground.

7.4 Shutdown

A timer follows the steady state sequence as soon as ignition ends. Once that timer reaches the desired cycle time, normally 30 or more minutes, the steady state sequence ends. Following steady state, the shutdown sequence occurs. During shutdown, the fan pressure setpoint remains the same as it was in steady state (0.35 inches of water), allowing any remaining fuel to burn the same as it had in steady state without changing the airflow. Two minutes after shutdown is initiated, the grinder turns on for thirty seconds. At this point, it is assumed that no burnable fuel remains in the chamber and only hot ash is sitting on the fuel grate. The thirty seconds of grinding ensures that as much ash as possible is removed so that the next burn can begin on an empty fuel grate.

7.5 Cycling

The shutdown sequence continues for 30 minutes, or until all of the thermocouples in the combustor are reading below 30°C, whichever is longer. During the tests that have been conducted thus far, 30 minutes has been more than enough time for the combustor to cool off as long as the exhaust fan is kept on. After shutdown is completed, the system looks to see if another burn has been requested. For a standalone combustor, this is simply a "cycle" switch in

the control system. In the full sanitation system, whether or not another burn begins will depend on either the available dry fuel load or the need to dry new incoming fecal material. If a cycle is requested, the fan shuts off and the startup sequence begins. If no cycle is requested, the fan power is cut and the system waits for a new burn to be initiated by the user or by the fecal drying system requesting a new burn.

CHAPTER 8: SECONDARY AIR TEST MATRIX

8.1 Secondary Test Matrix Hardware

To isolate the effect of secondary air hole size and orientation, a test matrix was created in which different secondary air inlet configurations were all tested under the same airflow and fuel feed rate conditions. To keep the tests as consistent as possible, mass flow controllers were used for air injection as opposed to the fan powered vacuum system. To complete the matrix, multiple separate secondary air inlet combustor sections were produced, and a quick disconnect flange connected the primary and secondary air sections. An image of one secondary inlet section can be seen below in Figure 21.

Figure 21: Secondary Air Module

To find the main fuel and airflow setpoints to test, the current (monofold) hole sizes for primary and secondary air were used with the forced air system. For this suite of tests, emissions were measured directly from the exhaust stream (as opposed to indirectly in the fume hood). This measurement technique was a new requirement by the gates foundation for emission standards, but also allowed for more accurate measurement of carbon monoxide levels, which were near the limit of detection during indirect measurement due to high combustion efficiency burns. The fuel feed rate and airflow rates with the unmodified secondary air hole configuration were modified over a series of tests to find the lowest average carbon monoxide (and by extension combustion efficiency) levels. The main difficulty of these tests was minimizing flame/combustion zone disruption during fuel additions. In every configuration, large spikes in carbon monoxide and drops in carbon dioxide production occurred during fuel additions. The steady state (between fuel additions) characteristics of the combustor were very consistent and exhibited modified combustion efficiencies above 99%. Therefore, reducing the effects of the fuel additions was a priority.

8.2 Secondary Modifications

To try and change the combustion characteristics, different secondary air hole configurations were designed to have different air flow velocities and flame sheet thicknesses. Smaller/less holes with the same amount of airflow would allow for much higher flow velocity. Multiple rows of properly sized holes would allow for the same injection velocities as the monofold/unmodified forced air system, while creating a much different air injection pattern. The main goal of modifying injection patterns and velocities was to achieve better mixing in the combustion zone, which has been shown to be the main driver of full carbon conversion to carbon dioxide (as opposed to carbon monoxide and unburned hydrocarbons).
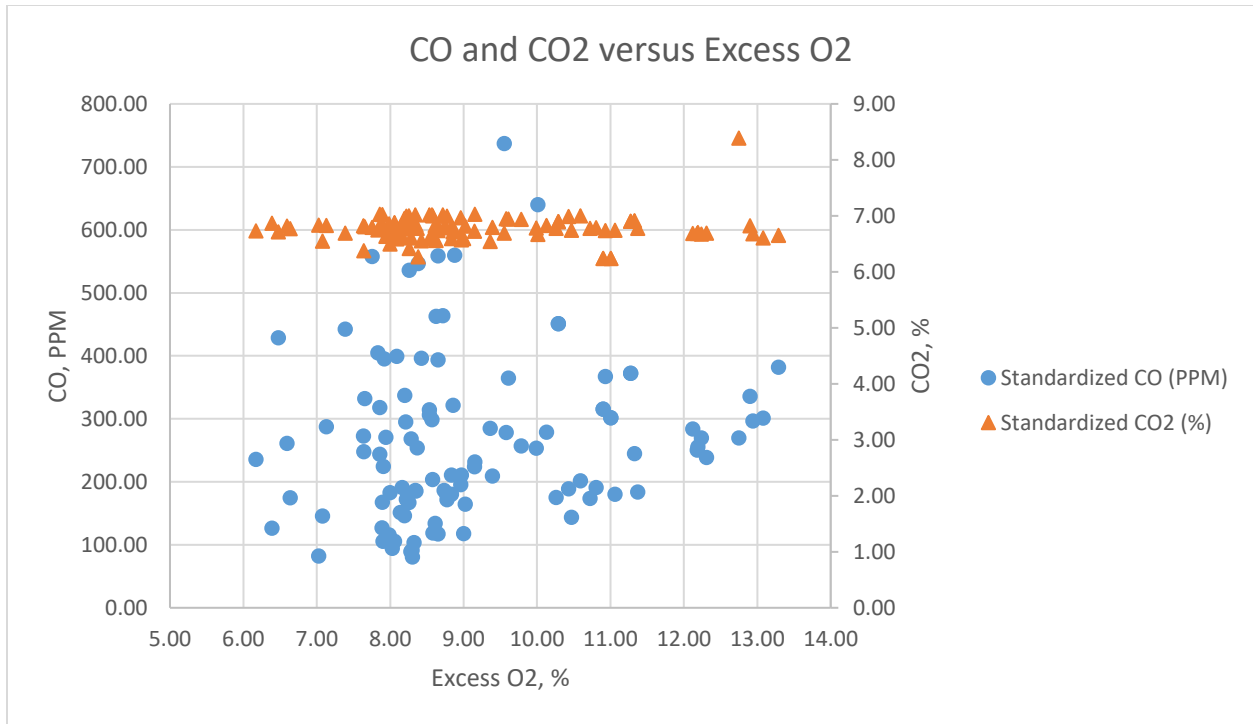
Figure 22: Combustor Emissions vs. Excess Oxygen Percentage
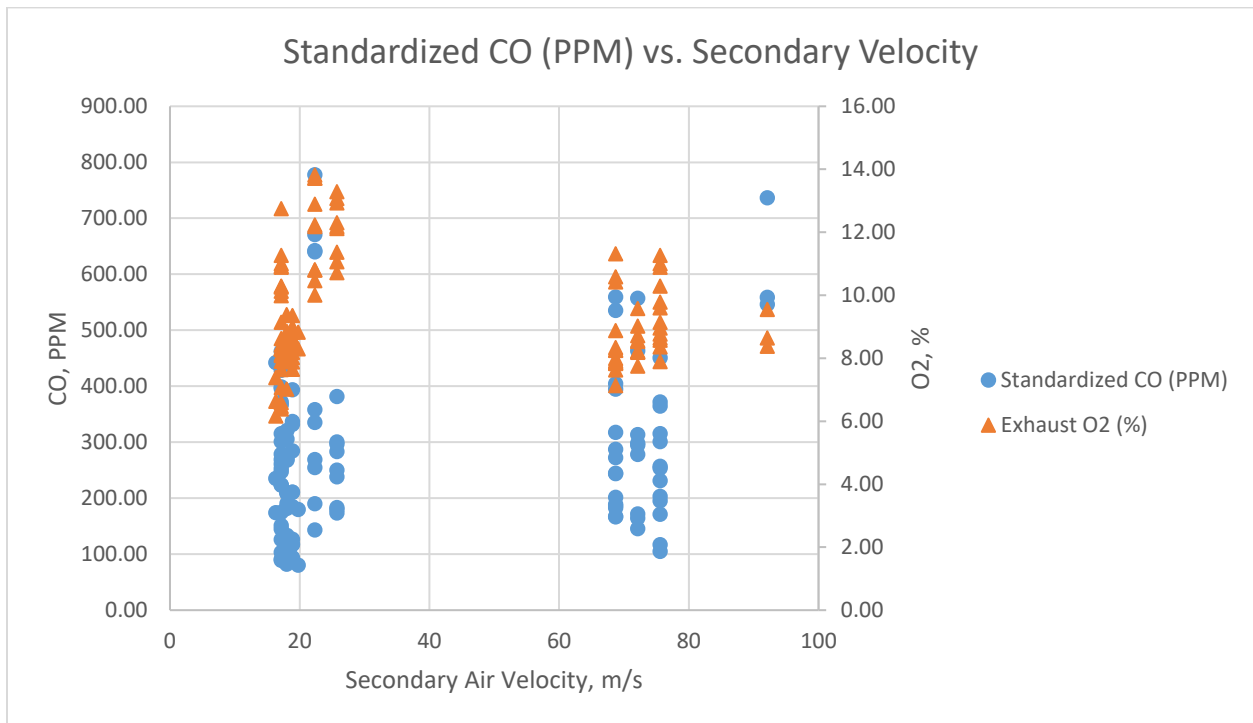
Figure 23: Emissions and Excess Oxygen vs. Secondary Air Inlet Velocity

8.3 Secondary Modification Performance

As can be seen in Figure 22 and Figure 23, the clear majority of secondary air hole geometries tested with mass flow controlled air had similar levels of carbon dioxide, while carbon monoxide and excess oxygen varied widely over the course of the test matrix. It is apparent that secondary air velocity doesn't substantially effect carbon monoxide emissions, which agrees with previous biomass combustion research that found sufficient mixing can occur within the range of 5 to 20 meters/second [16]. When compared to the original baseline test, the different hole geometries led to similar or increased carbon monoxide levels, indicating that burn performance was not improved by modifying hole geometries. This can be partially attributed to the original airflow setpoints and fuel feed rates tested on the secondary hole configurations being created/tuned with the original hole sizing. The emissions reduction from improvements in primary/secondary airflow rates and fuel timing can be seen below in Figure 24 and Figure 25, where primary and secondary airflow rates were changed in the original primary and secondary hole configurations. In these charts, the best preforming inlet flowrate/fuel feed combination is designated with an X marker.
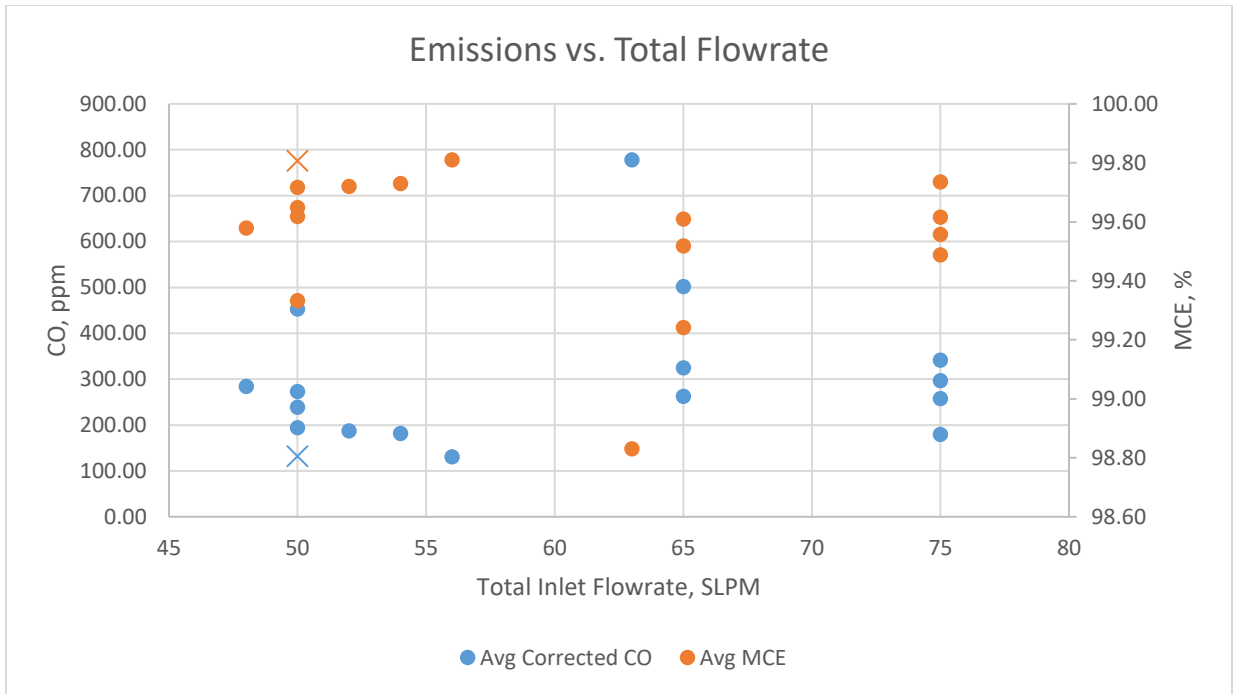
Figure 24: Combustor Emissions vs. Total Air Flowrate
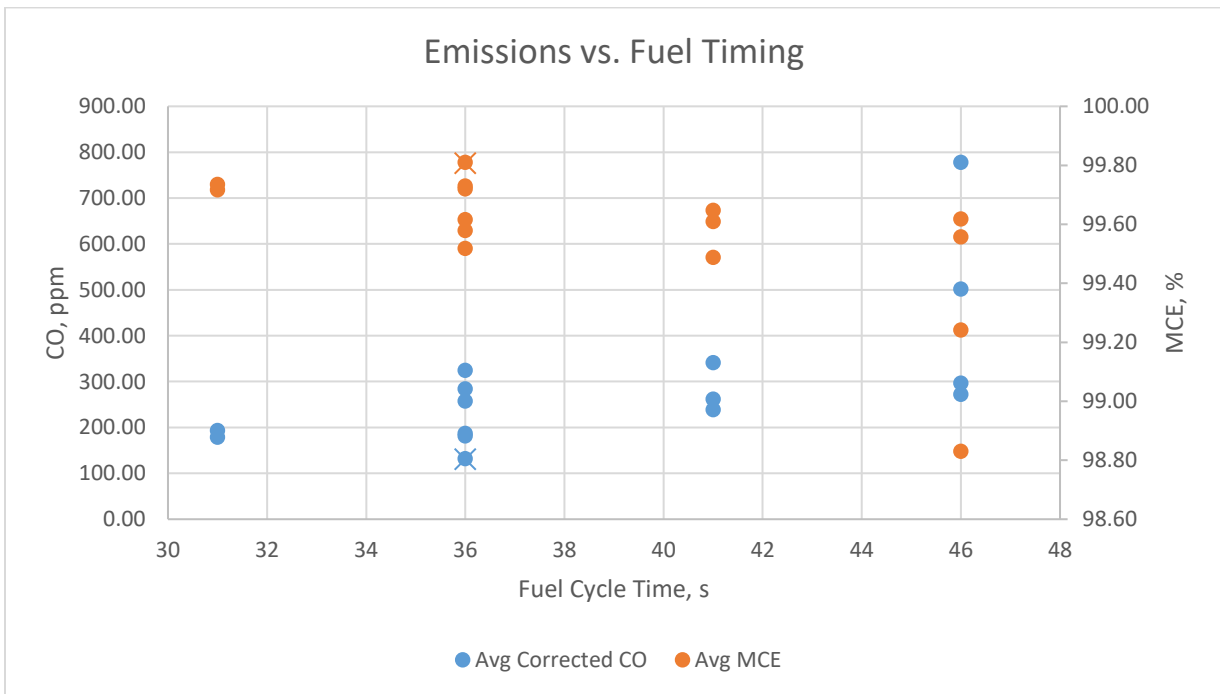
Figure 25: Combustor Emissions vs. Fuel Cycle Timing

These modified setpoints were used for all subsequent secondary air modification tests because preforming the full suite of tests on each secondary hole geometry was unrealistic given the time constraints and fume hood availability. One observation of testing was that secondary air velocities above 20 m/s tended to lead to worse emissions, as well as introducing the possibility of lofting small pieces of lit wood char. This behavior would likely carry over to fecal flakes as well, since they are less dense and have more surface area. Since fuel lofting can be highly damaging to the sensitive equipment downstream of the combustor, future hole modifications were designed to keep injection velocities below 20 m/s. The effects of multiple rows of holes with the same injection velocity (nominally 17 m/s) were minimal. As can be seen in Figure 26, most of the carbon monoxide, carbon dioxide, and excess exhaust oxygen levels were relatively similar between the multi-row and original single-row configuration. This again reinforces the idea that the main driver of emissions at this point was the effect of fuel additions on the hot fuel bed and flame region. The full secondary air test matrix can be found in Appendix A.
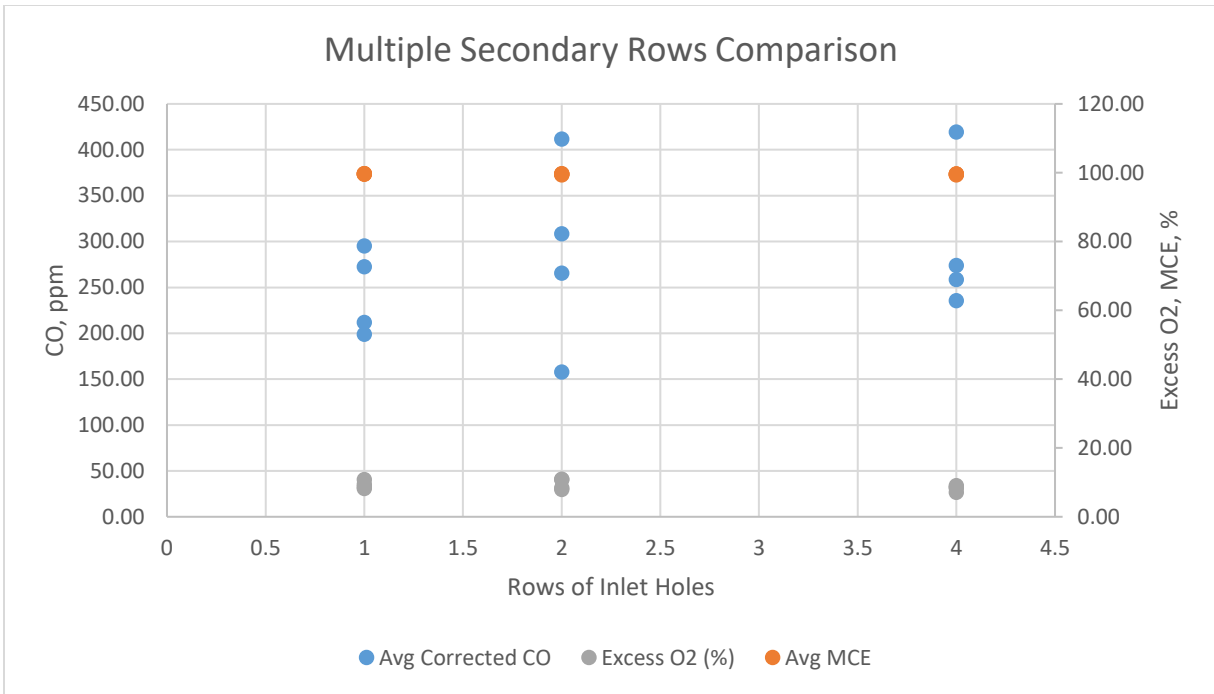
Figure 26: Multi-Row Secondary Inlets Comparison

8.4 Airflow Ratio Corrections

A thermocouple was also placed on the secondary air sheath to monitor the temperature of the injected air. This temperature helped to calculate the density differences in air injected between the primary and secondary holes, which allowed for the calculation of mass and volumetric flow rates during normal operation. Based off these numbers, the secondary inlet holes were enlarged slightly to maintain a true four to one ratio of secondary to primary air during steady state combustion. Due to the small change in hole size, emissions remained largely unchanged since the emissions during fuel addition are much worse than during steady state. The main method for reducing fuel addition emissions is to reduce size of fuel additions while increasing their frequency. The ideal fuel addition system would add the exact amount of fuel that was burning per second, while not disrupting the pyrolysis/flame zone.

CHAPTER 9: STARTUP TEST MATRIX

9.1 Startup Failures

As more human feces became available for burning/testing, it was apparent that the startup/ignition procedure that was effective for wood pellets was nowhere near consistent enough when igniting fecal flakes. While the feces would produce large amounts of syngas during every startup, it would tend to get stuck in a "smoldering" type of combustion where the entire fuel bed continually pyrolyzes at a low temperature without any flaming combustion occurring. For the entire system to be robust, every startup had to guarantee ignition and the transition to a steady state burn. While the control system does include contingencies for non-light or extinguish scenarios, those are reserved as a last resort in case of an unexpected event.

The most likely cause for the discrepancy in ignitability of feces stems from the differences in the donor's dietary habits and digestive efficiency. To counteract the variability of fecal fuels, a new ignition sequence was developed through a series of tests. Once the fuel is ignited and steady state is reached, there is little difference in the combustion performance of fecal fuels from different sources. Because of this the steady state sequence for fecal burns wasn't investigated/changed during these tests. Throughout these startup tests, wood was again used as a surrogate fuel many times to try and improve burn parameters without wasting the scarce fecal fuels we had available.

9.2 Startup Matrix Limitations

The main limiting factors in achieving a robust ignition sequence were combustor geometry and fuel availability. The allotted fecal material for startup testing was just over 700g, which would allow for approximately 23 startups (depending of fuel load). To ensure the fuel

didn't go to waste, an open top configuration of the monofold combustor was utilized. The

combustor was simplified by separating a combustion chamber from the rest of the system and

replacing the ash grinder section with a simple cap below the fuel bed. Mass flow controlled air

was fed into the monofold opening, as well as through the igniter entrance to allow for separate

modulation of the two air sources without changing the primary/secondary air ratio created by

the monofold enclosure. A quartz window was placed above the combustion chamber to allow

the fuel inside to be viewed by a camera during startup. The combustion chamber and camera

can be seen below in Figure 27.

Figure 27: Startup Test Setup

9.3 Ignition Techniques

The different ignition techniques applied include air ramping, sparking, and air pulsing. Ramp ignition included slowly ramping the air fed to the igniter and the monofold, at a set ratio of 4 SLPM through the monofold per 1 SLPM through the igniter. This ratio mimicked the approximate relative sizes of the igniter opening and the monofold opening. Spark ignition relied on a spark being introduced near or below the secondary air inlets during high syngas production to try and initiate flaming combustion. The third method of pulse ignition called for pushing a large amount of air through the air igniter for a short amount of time (<2 seconds) and then returning to its normal state for a longer period of time (4-6 seconds). To mimic the available hardware on the fan driven system, the air fed through the monofold was decreased whenever the igniter flow was increased. This acted as a surrogate for the monofold closure fluttering the monofold opening nearly closed while the igniter stayed open and the fan maintained a constant pressure in the chamber.

9.4 Ramp Ignition

The first new ignition sequence tested was to ramp the igniter and monofold air at a ratio of 1:4 at a set rate of 1-5 SLPM flow increase per minute. The ratio of air between the monofold and igniter was derived from the geometry ratio between the inlets. The igniter was also allowed a preheat period in these tests, to ensure that it was sufficiently hot once airflow began to not waste fan power. In this system, the wood loads consistently ignited the fastest when increasing flows by 3 SLPM per minute. However, when the ramp ignition was tested with fecal fuels, only 1 out of 7 loads ignited. The loads that did not ignite created huge plumes of syngas for over three minutes without any flame occurring. The load that did ignite consisted of 30 grams of fuel, whereas all previous tests had been based on 20g. In addition, the one fecal ignition to

succeed only did so immediately after the igniter air was cut off. These results led us to investigating other ways to ignite the syngas and ways to perturb the fuel be during ignition to promote flame formation.

9.5 Spark Ignition

Due to the huge volume of syngas created during a fecal startup, spark ignition of the syngas near the secondary air inlets was investigated next. To achieve a spark in the combustion zone, a metal rod was threaded through a small ceramic tube that was in turn threaded through a metal tube. The inner rod and outer metal tube acted as the electrodes for a generic stove spark system. When this system was tested during wood ignitions, the initial results seemed promising, although it was hard to tell since wood loads normally ignited rather quickly and consistently. Each wood test ignited while the spark was near the secondary air inlet, though it was hard to tell if it was from the spark or from the air igniter alone. When tested with fecal fuel, sparking was only able to ignite the fuel when the airflows were modulated as well. With this result and the previous ignition with modulating airflows, a feasible method of airflow modulation in the full combustor was investigated next.

9.6 Pulse Ignition

Since the full combustor system was operated by a fan and a single linear actuator to open/close the igniter, the air modulation couldn't be nearly as drastic as was possible with the mass flow controllers. To try and mimic possible scenarios for the full system, the mass flow controlled air was modulated by decreasing flow through the monofold while increasing it through the igniter. This simulated nearly closing the monofold opening, while leaving the igniter fully open. During these "pulse" tests, flow through the igniter was increased (and monofold air decreased) for one to two seconds, then brought back to the baseline levels for four

to six seconds. This cycle of igniter pulses was designed to allow the igniter to maintain high temperatures while consistently changing the airflow inside of the chamber to promote ignition. This series of tests ended up successfully lighting feces five times out of seven attempts with different fuel loads, airflows and pulse timings.

To further improve the pulse ignition sequence, wood fuels were again used to roughly dial in on the proper setpoints for pulse timings within a given fuel load and airflow. After the pulse timings were set, two more fecal ignitions were tested and succeeded within record time. With the pulse timings, fuel loads, airflow values, and igniter preheat parameters set, it was time to transition the ignition sequence to the full combustor system. This included converting the fuel load values to auger timings, airflows to fan voltages, and pulses to linear actuator setpoints. The door system between the monofold/igniter also had to be modified to allow the monofold door to nearly close while the igniter was fully open, creating the pulse of air through the igniter.

9.7 Grinding to Aid Ignition

Even with these settings copied from the forced air system, feces ignitions were only successful two times out of twelve attempts. It seemed that the fan/linear actuator could not respond quickly enough to create the drastic airflow changes that had occurred with the forced air pulses. Another likely culprit was the ash grinder blade, which at the time was untracked and could have been blocking or partially blocking the air igniter hole on multiple occasions. To fix this, the grinder blade was indexed so that it would always be perpendicular to the air igniter inlet hole, ensuring it wouldn't interfere with ignition. A grinding sequence was also added to the ignition sequence to further perturb the fuel bed during startup and hopefully stimulate flame formation. The grinder blade was rotated 180° at one to two minute intervals during startup, keeping it in the perpendicular position while introducing new fuel to the hot igniter air.

With the pulse and grind ignition procedure, five out of six fecal ignitions were successful. The final modification to startup involved adding the air ramp back, since the ramping with wood had proven to speed up the ignition process, not to mention that some level of ramping was inevitable with a fan driven system. This new ignition sequence has been able to light wood and fecal fuels with the exact same parameters, save for the amount of time it takes the auger to get similar fuel loads onto the fuel grate. This new startup procedure has proven itself to be quicker and, importantly, much more fuel independent that any of the previous startup schemes. The full test matrix of startups can be found in Appendix B.

9.8 Ignition Fuel Loads

To load enough fuel into the chamber before ignition can occur, the long shafted auger from RTI had to be run in excess of 200 seconds. The fuel piston system had to be run for at least 12 additions, which take at least 16 seconds per addition. During the original ignition sequence, a much faster auger was used, allowing the startup sequence to begin with simultaneous fuel additions and igniter preheating. To accommodate the slower fuel additions, a separate sequence was added prior to igniter preheating. In the new "pre-ignition" sequence, the fuel auger is activated by itself while the igniter and all other systems remain powered off. When there is less than twenty seconds (or one piston actuation cycle) of fuel additions left, the hot air igniter turns on and the ignition sequence begins as normal. The final bit of fuel needed for ignition is added as the igniter preheats, saving a few seconds in the ignition sequence.

As fuel additions change in subsequent combustor setups, the pre-ignition sequence may become unnecessary once again. If enough fuel for an ignition can be added while the igniter is heating up, i.e. thirty to sixty seconds, the control system will be reverted to not include the pre-

ignition sequence. Ideally, the fuel delivery system will introduce fuel quickly and consistently while consuming as little power as possible.

10.1 Full System Integration

With the full control system for startup, steady state, and shutdown completed and verified on the combustor system, the next logical step was to implement the controls on a full solid waste sanitation system. The control system's hardware and software were shipped out to Research Triangle Institute in North Carolina, where the full toilet prototypes are housed. The full system fecal path begins at a solid/liquid separator just below a squat plate. This separator moves all the non-liquid waste into a large piston driven retention cylinder. In this cylinder, the wet waste is collected and pushed through a macerator on its way to the drying plate interface. Loads of fecal material are extruded onto the drying plate whenever it has reached the required temperatures. The plate is heated by the combustor's hot exhaust tubes, which split just under the base of the plate, creating a larger conduction surface for heat transfer between the exhaust flow tube and the drying plate. A diagram of the fecal drying path can be seen below in Figure 28 [17].
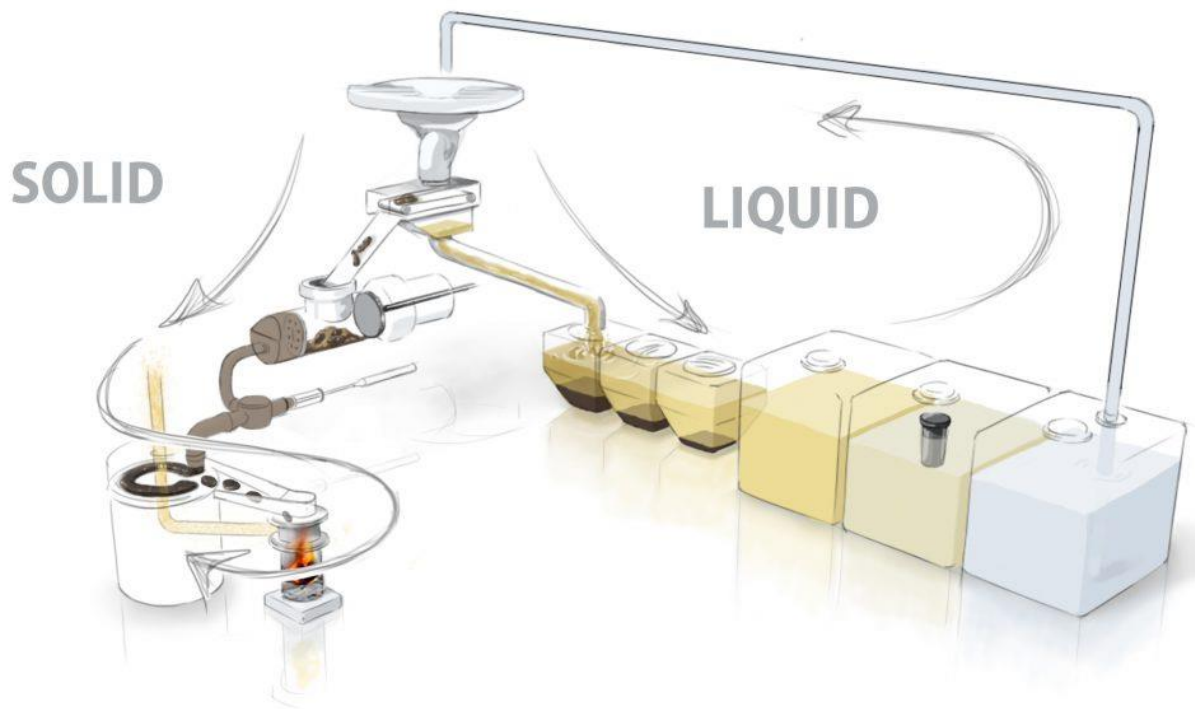
Figure 28: Solid and Liquid Sanitation Path

10.2 System Performance Metrics

The main points of interest when conducting burn tests on the full solid waste system were drying plate temperatures, fecal drying efficiency, fuel consumed by the combustor, and the amount of time it took for the combustor to reach drying temperatures. By measuring combustor firepower/fuel consumption rate, as well as the amount of time it takes to dry a set mass of feces, an overall heat conversion efficiency and fuel creation/consumption ratio can be calculated. A maximized heat conversion efficiency would mean that as much heat as possible is removed from the exhaust stream and applied to the drying feces. The ratio of fuel creation to consumption would need to be 1.0 or lower for the system to be energy independent. Anything higher than 1.0 means that the amount of fuel being dried is less than the amount of fuel it takes to dry it, and supplemental energy will be required for the system to run. A value below 1.0

means that some excess dry fuel is being created in addition to the fuel needed for drying wet material.

10.3 System Fueling Options

When the control system was being implemented at RTI, three separate types of fuel were available for testing. The main fuel used previously was human feces from employees/volunteers in North Carolina. The bulk of this sample had been manually dehydrated to reach (or nearly reach) zero percent moisture content. The second fuel available was feces from North Carolina that was dried on the plate dryer, which used heat from the combustor or in some cases supplemental heat from a heat gun collocated with the combustor. These feces were for all intents and purposes identical in composition to the other dehydrated feces used for combustion testing, but it had a wide range of moisture contents based on all of the variables surrounding the plate dryer when the fuel had been dried. The average moisture content for this fuel was ~30%. The last fuel tested was feces from the test site at the Centre for Environmental Planning and Technology (CEPT) University in Ahmedabad, India. These feces had been dried on the drying plate of an earlier prototype of the full system, but only used heat from the heat gun for fuel drying. These feces again had a wide range of moisture contents, but a sample of the properly dried material had an average moisture content of 3.64%.

10.4 System Controls

To run the full combustor system in North Carolina, the control software was run through a National Instruments USB 6001 multifunction I/O device (USB DAQ). This data acquisition device consists of multiple digital I/O ports, as well as two analog outputs and four analog inputs. With this hardware, every high voltage device (igniter, grinder, fuel auger) was run through relays that were switched on/off with the USB DAQ's digital outputs. The fan and

linear actuator voltage were both controlled via the analog outputs. The analog inputs enabled

the pressure measurements from the pressure transducer (1-5V output) to be recorded. The

thermocouple measurements needed to control the combustor were relayed through an Omega

USB data acquisition module, but for future builds a simple thermocouple amplifier will allow

the amplified thermocouple signal to be fed directly into the analog inputs of the USB 6001.

With this setup on the USB DAQ, the combustor was run with the same control software as the

device at CSU's testing facilities. The continuity of control software between the two test sites

allowed for good data comparisons between the different combustor systems.

10.5 Combustor Differences

The major differences between the combustor run at CSU and the one at RTI were the

fuel addition method and exhaust path routing. The fuel feed mechanisms at CSU consist of

either a long auger shaft with a small hopper at the feed end (RTI Auger) and the original CSU

auger. With both auger systems, the combustor side of the auger shaft drops fuel into a chute

that is slanted 50° to prevent fuel buildup. This chute enters the combustor a few inches above

the secondary air inlet holes. The system at RTI is fed with a ½ inch cylindrical piston located

below a fuel hopper. The forward motion of the piston pushes a small load of fuel into the

combustor, then the fully forwards position seals the end of the piston tube from pressure leaks.

Whenever the piston is not in/near the fully forwards position, substantial pressure leaks occur at

the pressure sensor, on the order of 0.1 inches of water. For these reasons, the piston fuel

feeding system had trouble keeping a consistent flame in the combustor.

The exhaust gases in the CSU combustor version are routed directly upwards from the

combustion chamber to the exhaust fan, with a three-foot section of uninsulated pipe to allow for

the gases to cool before passing through the fan. In the RTI system, the exhaust gas first hits a

90° elbow which reroutes the gasses towards the drying plate. The exhaust then turns another 90° upwards just underneath the plate, where it splits in a T junction located just underneath the drying plate. The two exhaust streams created at the T junction flow through smaller pipes than the rest of the exhaust stream in order to create hotter surface temperatures which can conduct to the drying plate more efficiently. Past the drying plate the exhaust rejoins into a single exhaust stream that is fed through the exhaust fan. The overall result of the complete exhaust system at RTI is that the exhaust fan has to work much harder to overcome the static pressure drop of the extra tubing. During normal burn cycles, the exhaust fan has difficulty keeping the pressure drop in the combustor above 0.3 inches of water. The coupled effect of exhaust routing and fuel piston actuation creates relatively low, highly fluctuating pressure differentials inside of the combustor.

10.6 Full Control System Burns

One concern of the differing fuel moisture contents and compositions was that they would be difficult or unable to light with the ignition sequence that was designed for a single fuel type. Luckily, the combination of igniter pulsing, grinder position/rotations, and delta pressure ramping during startup was able to light every type of fuel available. The only difference between startups of the different fuels was the amount dropped onto the fuel grate prior to ignition. The control system also differed in how it transitioned to steady state for the different fuels by waiting for the lowest thermocouple to detect higher or lower temperatures after ignition before subsequent fuel additions occurred. This waiting period proved useful for the less energetic fuels (moist feces), as it allowed a stronger flame to develop over the starting fuel load before any fuel was dropped on could potentially put the flame out. With more energetic fuels (dry feces, wood pellets), this starting period wasn't nearly as necessary as their flames were

more stable in general, and waiting longer period of time to add fuel would simply increase the time it took for the combustor and drying plate to reach operational drying temperatures.

10.7 Fecal Drying

In order for the plate drying sequence to begin with the full combustor assembly, the temperature in the enclosed space just above the plate dryer was monitored. Once this temperature reached the desired temperature, wet fecal material was applied and dried for 22 minutes before being scraped off so that another fecal drying sequence could begin. The moisture content of the freshly dried feces varied greatly with the different fuel types and their burn characteristics. With wood pellets, temperatures remained high for the entire test, the flame never seemed to extinguish, and all of the fecal material that was applied to the plate dryer came off with very low moisture content. When using fully dehydrated fecal material to run the combustor, similar temperatures were achieved with a much higher fuel feed rate. Temperature fluctuations were still present, but the amount of heat produced and flame stability were still enough to create a very low moisture content fuel through drying. Whenever the fecal material with higher moisture contents was burned, the flame was unable to stay lit for the entirety of the period between fuel additions. The flame instability caused lower overall temperatures and thus the fecal material that was being dried ended up with higher moisture content than the other tests, and the fuels created had a higher variance of moisture content. The only drying cycles to create low moisture content fuel with Indian feces were manually fed more fuel than the piston system was capable of delivering. During the "excess fuel" test, the combustor heated to operating temperatures within 30 minutes, as opposed to the hour it took during normal fuel feeding. For these reasons, a faster fuel feed rate/mechanism was deemed necessary for higher moisture content/lower energy content fuels.

CHAPTER 11: HEALTH AND ENVIRONMENTAL IMPACT

11.1 Production of Harmful Emissions

When discussing the combustor's design and control sequences, it is important to frame the entire project from a health and emissions standpoint. Since the main purpose of the RTTC is to reduce disease and improve lives, any negative heath impact caused by the system should be heavily investigated to ensure that we aren't just replacing one problem with another. While burning fecal material is one of the quickest ways to destroy pathogens and disease causing bacteria, it has the major drawback of producing carbon emissions just like any other combustion process. While the cookstoves team strived to reduce and improve emissions as much as possible, carbon dioxide and small amounts of other emissions will enter the atmosphere after passing through the full system. The best we can do is ensure that as much carbon as possible fully converts to carbon dioxide, which is much less damaging to the environment than the other possible carbon emissions. Carbon monoxide and other unburned hydrocarbons can exist in the system if the air to fuel ratio isn't adequate, or if the air-fuel mixing near the flame zone isn't thorough enough to introduce oxygen to all the fuel particles.

11.2 Particulate Emissions Comparison

To evaluate the health impact of the gates combustor, we have compared the combustor's emissions to other gasifier/stove emissions standards when using wood pellets. As there are no fecal fuels that are regularly tested for particulate and gaseous emissions, we have little choice but to assume that preforming well against other continually-fed wood burning stoves indicates the combustor would perform just as well against others burning fecal material. As can be seen below in Figure 29, the particulate emission rate of the combustor when burning wood pellets is

in line with the cleanest EPA certified pellet stoves/heaters. Particulate matter emitted from the system tends to be in the respirable range below 2.5 µm, where the particulate can enter and deposit in the alveolar region of the lungs and cause both acute and long-term health effects including cancer [18]. While particulate matter cannot be eliminated from these systems, emissions have been reduced at every available opportunity to try and mitigate total system health impact.
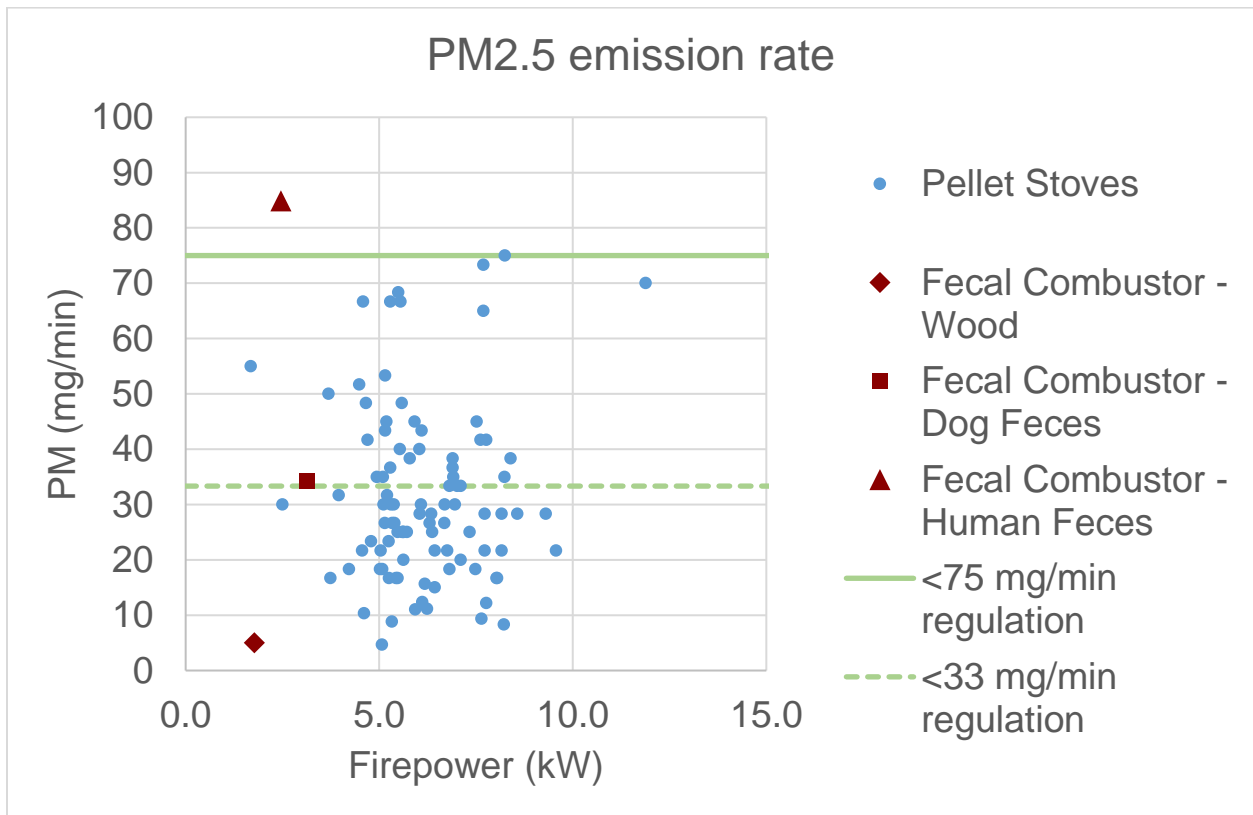
Figure 29: Pellet Stove Emissions Comparison

11.3 Emissions Comparison Limitations

The data for human and canine feces shown above represent a near worse-case scenario for particulate emissions, as the data was taken before the fuel and air flowrates were improved for either fuel. The combustor setpoints used for those tests help to ensure a very stable and robust burn, but don't reflect all the subsequent emissions improvements that occurred over the

course of combustor improvements. It is also important to note that the combustor runs at a lower firepower than most of the commercial stoves it is compared to. This low firepower was designed more for fuel conservation than low emissions, and it is fully expected that a similarly efficient could be created to run at a higher firepower since scaling combustion up has proven itself to be much easier than scaling it down.

11.4 Modified Combustion Efficiency

The other major metric used to judge the performance of the stove is modified combustion efficiency (MCE). MCE is a calculation of carbon conversion to carbon dioxide, meaning any carbon monoxide or other higher order carbon molecules that did not fully react with oxygen reduce the system's overall MCE. The calculation of MCE is shown below in Equation 6 [19].

<div align="center">Equation 6: MCE Calculation</div>

$$MCE = \frac{\Delta CO_2}{\Delta CO_2 + \Delta CO}$$

$$\Delta X = X_{exhaust} - X_{background}$$

When wood pellets are burned in the combustor, MCE tends to be above 99 percent unless ignition is occurring, when carbon is escaping through unburnt syngas. In fact, carbon monoxide emissions were near the limit of detection in the powerhouse's gaseous emission measurement system whenever the combustor was in between fuel additions. Figure 30 and Figure 31 below show the modified combustion efficiency for wood pellets and for human fecal material, respectively. Note that the y axis minimum is 90% modified combustion efficiency, where 90 percent of all carbon in the exhaust stream converted completely to carbon dioxide.
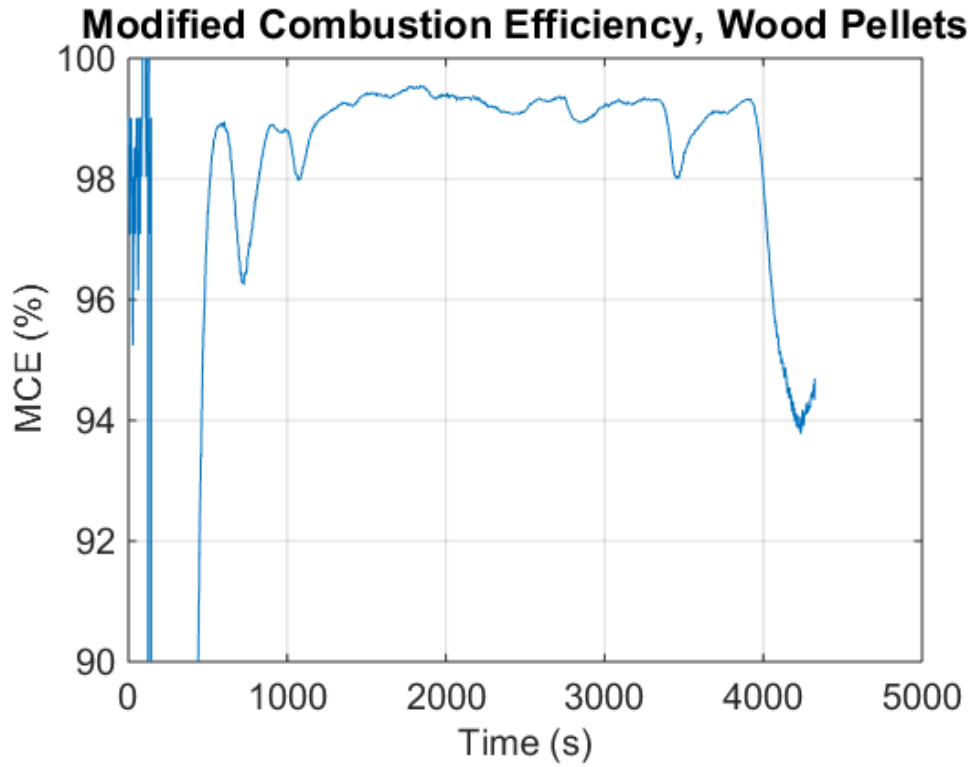
Figure 30: MCE for Wood Pellets
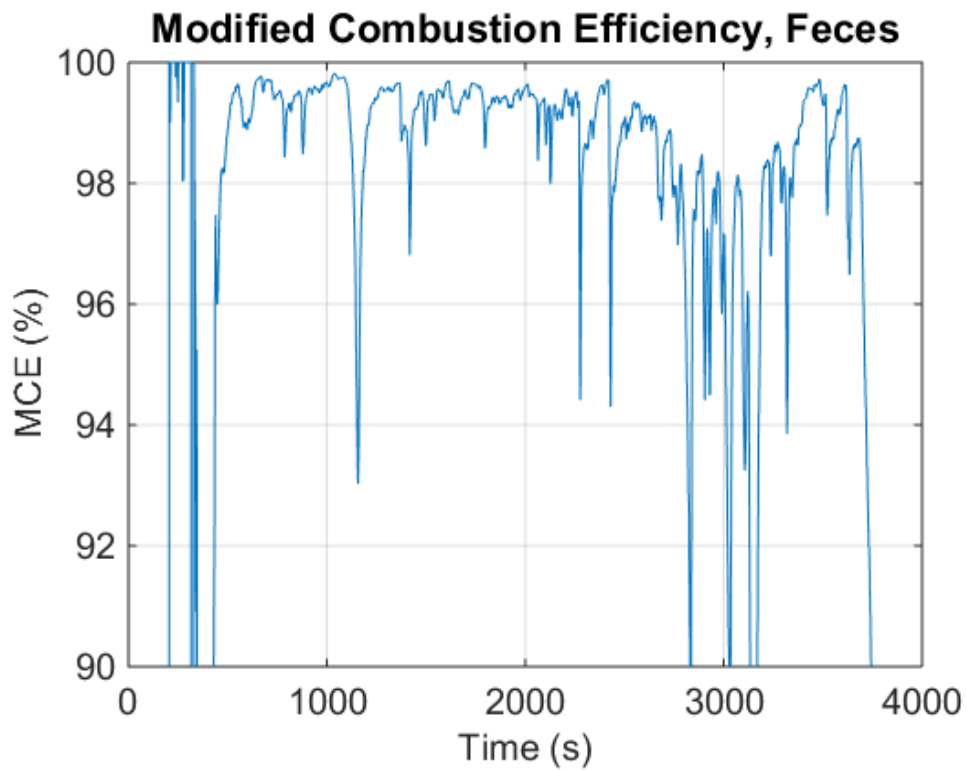
Figure 31: MCE for Human Feces

11.5 Greenhouse Effects

Another important health aspect of the combustor is the height at which emissions are released. While most commercial cookstoves are designed to exhaust directly onto a pot/cooking surface near ground level, the Gates combustor has a fully sealed exhaust stream that is only enters the surrounding air around 8 feet off the ground. At this height, the hot exhaust gasses are out of the directly breathing zone for anyone around the toilet system, and the latent heat in the exhaust creates a buoyant force from the cooler surrounding air to carry the exhaust even farther from any human respiratory system before it can enter back into the respirable zone. Because of these mitigating factors, large-scale greenhouse gas effects should be heavily evaluated, in addition to the more immediate damaging impact of particulate matter and carbon monoxide emission.

From Figure 9 in section 7.2, the exhaust of the combustor is known to contain an average of seven to eight percent carbon dioxide by volume, which is the major greenhouse pollutant created in the combustor. With the comparison of direct and indirect emissions measured from the combustor (Appendix C), the stove flowrate was calculated to be between 80 and 110 standard liters per minute (a mass measurement). As a worst-case carbon dioxide emission calculation, the stove exhaust flowrate can be estimated as 110 standard liters per minute, as shown in Equation 7.

Equation 7: Mass to Volumetric Flow Conversion

$$Flow\ (LPM) = Flow\ (SLPM) * \frac{T_{gas}}{294.26} * \frac{14.696}{P_{gas}}$$

With the gaseous emissions being measured at 503.15K and 12.3 psia, the volumetric flow of the stove when measured is 225 liters per minute. At ten percent of total exhaust gas composition, the flow of carbon dioxide out of the stove is 22.5 liters per minute. This equates

to 1350 liters of carbon dioxide per hour, or 1.35 m^3 per hour. The density of carbon dioxide at this temperature and pressure is close to (but less than) 1 kg/m^3. Thus, the combustor will produce an estimated maximum of 1.35 kg of carbon dioxide per hour. In this hour, the combustor will burn through 20 individuals (low income basis) to 28 individuals (high income basis) fecal material [10]. For reference, burning one gallon of gasoline in a vehicle will produce around 8.9 kg of carbon dioxide, and each mile driven produces 0.4 kg of carbon dioxide [20]. This means that the combustor can burn for six and a half hours, consuming 120-180 individuals' fecal material, while producing the same amount of carbon dioxide as a single gallon of gasoline.

A comprehensive calculation of exhaust flows, conducted in Matlab, can be seen in Appendix F.

11.6 Lifecycle Emissions

To calculate the total emissions from the sanitation system, the data for fuel constituents is extrapolated to the total 2.5 billion whom lack access to modern sanitation. The effective total yearly emissions of the different chemical components can be seen in Equation 8 thru Equation 10 below. The weights calculated are taken from the ultimate analysis of human feces from RTI, as they had the highest (worst case) sulfur content.

Equation 8: Yearly Dry Feces Creation

$$Total\ Yearly\ Feces\ (dry) = 2{,}500{,}000{,}000 * 38\frac{g}{day} * 365\frac{day}{year} = 34.68\frac{Tg}{year}$$

Equation 9: Yearly Fecal Carbon Emission

$$Yearly\ Carbon\ Emission = 34.68\frac{Tg}{year} * 0.4885\frac{g\ C}{g\ fuel} = 16.94\frac{Tg}{year}$$

Equation 10: Yearly Fecal Sulfur Emission

$$Yearly\ Sulfur\ Emission = 34.68\frac{Tg}{year} * 0.0091\frac{g\ S}{g\ fuel} = 315.6\frac{Gg}{year}$$

66

Carbon and sulfur, which readily form carbon dioxide and sulfur dioxide when burned, were considered the most damaging emissions from the system for this analysis. The release/formation of sulfur oxides is highly damaging to lung function, can cause premature mortality, and can lead to the destruction of vegetation [21]. A full exhaust characterization is underway to determine the conversion of sulfur to sulfur dioxide and possibly higher order chemicals (SO_3, H_2SO_4, etc). The characterization will include a full chemical analysis to find any other potentially harmful constituents in the exhaust stream.

To put these numbers in perspective, gasoline consists of 87% carbon by mass, and weighs about 2.86 kg per gallon. The carbon trapped in 2.5 billion individual's feces is therefore equivalent to 6.8 billion gallons of gasoline per year, whereas in the United States, an average of 143.37 billion gallons of gasoline are consumed per year [22]. Thus, the yearly carbon contribution of worldwide feces burning should fall within 4.7% of U.S. gasoline emissions.

For sulfur, the total U.S. emission of SO_2 from power plants in 2010 was 13 million tons per year, with half that weight coming from sulfur, and the other half oxygen [23]. That equates to 5.897 Tg of fuel-bound sulfur entering the atmosphere from power plants in the U.S. This makes the yearly sulfur emissions from 2.5 billion individual's feces is 5.35% of U.S. power plant emissions. In recent years, SO_2 emission has dropped to around 2 million tons per year (due mostly to the reduced use of coal), which make the fecal share of sulfur around 33% of power plant release. Because of this potential impact, the sulfur emission on the fecal sanitation system will likely have to be treated to prevent release to the atmosphere.

CHAPTER 12: CONCLUSIONS

12.1 Combustor Progress

The gates combustor system has gone through numerous modifications and iterations since its inception in early 2012. The fickle nature of fecal drying and combustion drove the development of innovative and novel methods of biomass ignition and combustion devices. The final system (as of this publication) is a fully automated, continuous feed, updraft semi-gasifier that is designed to work in a full sanitation system without connections to external power. The combustor burns multiple different types of fuels in a highly efficient and robust process that includes minimal power draw and heat waste. The combustor's flexibility in terms of size and power opens many possible future applications.

12.2 Energy Balance

In the near term, the teams at CSU and RTI will work to get the full toilet system closer to a mass balance at or below 1.0. Simple changes such as adding a solar panel or other supplemental energy sources could drastically simplify the problem, but for now all parties involved are focused on getting the feces drying and urine sanitation processes as efficient as possible. The next major step energy-wise will be adding a small steam engine and generator in the exhaust path to convert excess thermal energy to electrical energy. This electrical energy will then be used to run the combustor and the rest of the toilet system, including the electrochemical cells used for urine sanitation. While the system currently meets the challenge metrics of germ removal, user cost per day, and resource recovery, it will not be truly off-grid until mass balance has fallen below 1.0.

REFERENCES

[1]   Bill & Melinda Gates foundation, "Water, Sanitation & Hygiene - Bill &
        Melinda Gates Foundation." [Online]. Available: http://www.gatesfoundation.org/What-
        We-Do/Global-Development/Water-Sanitation-and-Hygiene. [Accessed: 27-Feb-2017].

[2]   L. Yermán et al., "Smouldering combustion as a treatment technology for faeces:
        Exploring the parameter space," Fuel, vol. 147, no. March, pp. 108–116, 2015.

[3]   J. Jetter et al., "Pollutant Emissions and Energy Efficiency under Controlled Conditions
        for Household Biomass Cookstoves and Implications for Metrics Useful in Setting
        International Test Standards."

[4]   N. Loveldi, "Development of a solid human waste semigasifier burner for use in
        developing countries," 2014.

[5]   A. Bhavanam and R. C. Sastry, "Biomass Gasification Processes in Downdraft Fixed Bed
        Reactors : A Review," Int. J. Chem. Eng. Appl., vol. 2, no. 6, pp. 425–433, 2011.

[6]   J. H. Wang, C. Y. H. Chao, and W. Kong, "Experimental study and asymptotic analysis of
        horizontally forced forward smoldering combustion," Combust. Flame, vol. 135, no. 4, pp.
        405–419, 2003.

[7]   C. Higman, M. van der Burgt, C. Higman, and M. van der Burgt, "Chapter 3 – The
        Kinetics of Gasification and Reactor Theory," in Gasification, 2008, pp. 33–45.

[8]   C. Higman and M. van der. Burgt, "Detailed Gasification Chemistry," 2008. [Online].
        Available: https://www.netl.doe.gov/research/coal/energy-
        systems/gasification/gasifipedia/gasification-chemistry. [Accessed: 26-Apr-2017].

[9]   S. E. R. Institute, T. B. Reed, and U. S. D. of Energy, "A Survey of Biomass
        Gasification," vol. II, no. 2. c., 1979.

[10]   C. Rose, A. Parker, B. Jefferson, and E. Cartmell, "The Characterization of Feces and
        Urine: A Review of the Literature to Inform Advanced Treatment Technology.," Crit.
        Rev. Environ. Sci. Technol., vol. 45, no. 17, pp. 1827–1879, 2015.

[11]   D. Vamvuka, N. El Chatib, and S. Sfakiotakis, "Measurements of ignition point and
        combustion characteristics of biomass fuels and their blends with lignite," Combustion,
        vol. 2015, no. April, p. 95, 2011.

[12]   T. Onabanjo et al., "An experimental investigation of the combustion performance of
        human faeces," Fuel, vol. 184, no. November, pp. 780–791, 2016.

[13]   G. Rein, "Smouldering Combustion Phenomena in Science and Technology," Int. Rev.
        Chem. Eng., vol. 1, no. January 2009, pp. 3–18, 2009.

[14]   Rauschert, "Rauschert Pellet stove igniter." [Online]. Available: http://www.rauschert-
        igniter.com/. [Accessed: 27-Apr-2017].

[15]   T. Onabanjo et al., "Energy recovery from human faeces via gasification: A
        thermodynamic equilibrium modelling approach," Energy Convers. Manag., vol. 118, no.
        June, pp. 364–376, 2016.

[16]   K. Dischino, "Methods for Particulate Matter Emissions Reduction in Wood Burning
        Cookstoves," 2015.

[17]   RTI International, "A Better Toilet | For A Cleaner World." [Online]. Available:
        http://abettertoilet.org/. [Accessed: 23-Mar-2017].

[18]   D. Upadhyay, V. Panduri, A. Ghio, and D. W. Kamp, "Particulate Matter Induces

Alveolar Epithelial Cell DNA Damage and Apoptosis Role of Free Radicals and the Mitochondria."

[19]   N. L. Briggs *et al.*, "Method to Calculate Modified Combustion Efficiency and its Uncertainty Supplement to: Particulate Matter, Ozone, and Nitrogen Species in Aged Wildfire Plumes Observed at the Mount Bachelor Observatory."

[20]   O. US EPA, "Greenhouse Gas Emissions from a Typical Passenger Vehicle."

[21]   World Bank Group, "Sulfur Oxides," *Pollut. Prev. Abat. Handb.*

[22]   U.S. Energy Information Administration, "How much gasoline does the United States consume? - FAQ - U.S. Energy Information Administration (EIA)." [Online]. Available: https://www.eia.gov/tools/faqs/faq.php?id=23&t=10. [Accessed: 30-May-2017].

[23]   "Power Plant Emission Trends | Clean Air Markets | US Environmental Protection Agency." [Online]. Available: https://www3.epa.gov/airmarkets/progress/datatrends/index.html. [Accessed: 30-May-2017].

Combustor	Test Number	Test Case #	Sec. Hole size (mm)	Rows of holes	Secondary Air Velocity (m/s)	Sec/Pri ratio	Primary Flow	Secondary Flow	Total flow (slpm)	Fuel cylce time (s)	Replicates (15 min)	Excess O2 (%)	Avg Corrected CO	Avg MCE
Micro V3	A.13.1	1	4	1	22.32	4.00	13	52	65	46	4	12.81	501.97	99.24
	A.11.1	2	4	1	22.32	4.73	11	52	63	46	1	13.72	777.93	98.83
	A.15.1	3	4	1	25.76	4.00	15	60	75	46	1	12.94	296.77	99.56
	A.10.1	4	4	1	17.17	4.00	10	40	50	46	4	11.02	272.65	99.62
	A.15.2	5	4	1	25.76	4.00	15	60	75	41	2	13.19	341.43	99.49
	A.15.3	6	4	1	25.76	4.00	15	60	75	36	3	12.20	257.52	99.62
	A.13.2	7	4	1	22.32	4.00	13	52	65	41	2	12.22	238.29	99.61
	A.10.2	8	4	1	17.17	4.00	10	40	50	41	2	9.57	238.64	99.65
	A.10.3	9	4	1	17.17	4.00	10	40	50	36	6	8.19	131.99	99.81
	A.10.4	10	4	1	17.17	4.00	10	40	50	31	2	6.49	193.86	99.72
	A.13.3	11	4	1	22.32	4.00	13	52	65	36	3	10.43	324.86	99.52
	A.15.4	12	4	1	25.76	4.00	15	60	75	31	3	11.05	179.17	99.74
	A.10.5	13	4	1	16.31	3.80	10	38	48	36	3	6.73	284.25	99.58
	A.10.6	14	4	1	18.03	4.20	10	42	52	36	6	8.22	187.14	99.72
	A.10.7	15	4	1	18.89	4.40	10	44	54	36	5	8.52	181.88	99.73
	A.10.8	16	4	1	19.75	4.60	10	46	56	36	2	8.57	130.41	99.81
Micro V2	B.10.1*	17*	2	1	68.69	4.00	10	40	50	36	3	8.21	453.17	99.33
	B.10.2*	18*	2	1	72.12	4.20	10	42	52	36	3	8.86	614.16	99.07
	B.10.1**	17	2	1	68.69	4.00	10	40	50	36	3	7.54	292.77	99.57
	B.10.2**	18	2	1	72.12	4.20	10	42	52	36	3	8.33	339.02	99.50
	B.10.3**	19	2	1	75.56	4.40	10	44	54	36	3	8.31	158.84	99.77
	B.10.1***	17	2	1	68.69	4.00	10	40	50	36	3	8.03	199.23	99.72
	B.10.2***	18	2	1	72.12	4.20	10	42	52	36	3	8.61	358.88	99.49
	B.10.3***	19	2	1	75.56	4.40	10	44	54	36	3	8.83	202.18	99.71
	B.10.1HO	17	2	1	68.69	4.00	10	40	50	36	3	10.78	211.84	99.70
	B.10.1	17	2	1	68.69	4.00	10	40	50	36	3	8.17	295.31	99.55
	B.10.2	18	2	1	72.12	4.20	10	42	52	36	3	8.66	198.89	99.72
	B.10.3	19	2	1	75.56	4.40	10	44	54	36	3	9.45	272.39	99.61
Secondary E	E.10.1.HO	26	2.83	2	17.15	4.00	10	40	50	36	2	10.95	308.46	99.51
	E.10.1	26	2.83	2	17.15	4.00	10	40	50	36	2	10.78	411.71	99.41
	E.10.2	26	2.83	2	18.01	4.20	10	42	52	36	3	8.39	157.80	99.77
	E.10.3	26	2.83	2	18.87	4.40	10	44	54	36	3	7.91	265.48	99.61
Secondary G	G.10.1	28	2	4	17.17	4.00	10	40	50	36	3	7.06	273.97	99.59
	G.10.2	28	2	4	18.03	4.20	10	42	52	36	3	8.63	258.55	99.62
	G.10.3	28	2	4	18.89	4.40	10	44	54	36	3	9.05	235.52	99.64
	G.10.1-2	28	2	4	17.17	4.00	10	40	50	36	3	8.38	419.30	99.37

Test Number	Desc.	Fuel Type	Test Type	Fuel Loading	Air Ramp	Air Pulse	Pulse Timing	Air Ratio	Igniter Preheat	Time to Ignition	Adjusted Ign. Time
BB-4		Wood	Ramp	20g	3	X	X	4.0	1:00	4:14	3:14
BB-5		Wood	Ramp	20g	3	X	X	4.0	1:00	4:18	3:18
BB-6		Wood	Ramp	20g	3	X	X	4.0	1:00	4:30	3:30
BB-7		Wood	Ramp	20g	3	X	X	4.0	1:00	4:23	3:23
T2-2	Fast Ramp	Wood	Ramp	20	1	X	X	4.0	1:00	2:19	1:19
T2-3		Wood	Ramp	20	3	X	X	4.0	1:00	3:19	2:19
BB-7-2		Wood	Ramp	20	3	X	X	4.0	1:00	2:41	1:41
BB-8	Hi Fuel	Wood	Ramp	40	3	X	X	4.0	1:00	2:14	1:14
BB-9	Lo Fuel	Wood	Ramp	15	3	X	X	4.0	1:00	3:03	2:03
BB-10	Lo Ratio	Wood	Ramp	20	3	X	X	2.5	1:00	3:05	2:05
BB-11	Hi Ratio	Wood	Ramp	20	3	X	X	5.5	1:00	2:48	1:48
BB-12	Fast Ramp	Wood	Ramp	20	1.5	X	X	4.0	1:00	3:32	2:32
BB-13	Fast Ramp	Wood	Ramp	20	1.5	X	X	4.0	1:00	3:18	2:18
BB-14	Slo Ramp	Wood	Ramp	20	4.5	X	X	4.0	1:00	2:58	1:58
BB-15	Feces Ramp	Feces	Ramp	20	3	X	X	4.0	1:00	NA	NA
BB-16		Feces	Ramp	20	1	X	X	4.0	1:30	NA	NA
BB-17		Feces	Ramp	20	1	X	X	4.0	1:00	NA	NA
BB-18	Kill Ign Air	Feces	Ramp	30g	1	X	X	4.0	1:00	4:07	3:07
BB-19	Ign Ramp	Feces	Ramp	20	3	X	X	4.0	1:00	NA	NA
BB-20	Ign Set	Feces	Ramp	20	1	X	X	4.0	1:00	NA	NA
BB-21	No Pre	Feces	Ramp	20	3	X	X	4.0	0:00	NA	NA
BB-22	DBL Set	Wood	Set	30?	NA	X	X	4.0	0:00	2:50	2:50
BB-23	Dbl Set	Wood	Set	30?	NA	X	X	4	0:00	1:50	1:50
BB-24	Ign Only	Wood	Set	30?	NA	X	X	NA	1:00	3:15	2:15
BB-25	Pulse Off	Wood	Pulse	30?	1	0_45	3s each	4	1:00	Unknown	Unknown
BB-25-2	Pulse John	Wood	Pulse	20?	NA	20_36	5 sec PW	4	1:00	2:48	1:48
BB-26	Pulse Max	Wood	Pulse	20?	3	20_36	1 on 5 off	4	1:00	3:12	2:12
BB-27	Pulse Max	Feces	Pulse	20	3	20_36	2 on 5 off	4	1:00	3:40	2:40
T2-6	Spark1	Wood	Ramp-Spark	20	3	NA	Spark at 1m	4	1:00	3:20	2:20
T2-7	Spark2	Wood	Man Spark	20	3	NA	Spark at 2m	4	1:00	NA	NA
T2-9	Spark2.2	Wood	Set Spark	20	3	NA	Spark at 2m	4	1:00	2:15	1:15
T2-10	Spark3	Feces	Man Spark	20	NA	Manual_20	Spark at 2m	4	1:00	4:00	3:00
T2-11*	Pulse Mess	Wood	Pulse	20	2	20	2 on 5 off	4	0:30	2:30	2:00
T2-12		Wood	Pulse	20	2	20	2 on 5 off	4	0:30	2:17	1:47
T2-14		Wood	Pulse	20	2	20	3 on 5 off	4	0:30	2:53	2:23
T2-15		Wood	Pulse	20	2	20	3 on 5 off	4	0:30	2:40	2:10
T2-16		Wood	Pulse	20	3	20	2 on 5 off	4	0:30	2:33	2:03
T2-17	Feces Pulse	Feces	Pulse	20	3	20	2 on 5 off	4	1:00	3:40	2:40
T2-18		Feces	Pulse	20	2	20	2 on 5 off	4	1:00	NA	NA
T2-19		Feces	Pulse	20	3	20	2 on 5 off	4	1:00	3:22	2:22
T2-20		Feces	Pulse	20	3	20-25	2 on 5 off	4	1:00	NA	NA
T2-21		Feces	Pulse	40	3	20	2 on 5 off	4	1:00	4:30	3:30
T2-22		Feces	Pulse + Man	40	2	20-80	2 on 5 off	4	1:00	6:25	5:25
T-23	Pulse Mods	Wood	Pulse	20	2	20	0.5 on 0.5 off	4	0:30	2:40	2:10
T-24		Wood	Pulse	20	2	20	1 on 1 off	4	0:30	3:02	2:32
T-25	Baseline	Wood	Ramp	20	2	X	X	4	0:30	2:30	2:00
T-26	Pulse Mods	Wood	Pulse	20	2	20	0.5 on 1 off	4	0:30	3:14	2:44
T-27		Wood	Pulse	20	2	20	2 on 1 off	4	0:30	2:35	2:05
T-28?		Wood	Pulse	20	2	20	2 on 4 off	4	0:30	2:29	1:59
T-28-2		Wood	Pulse	20	2	20	1 on 4 off	4	0:30	2:16	1:46
T-29		Wood	Pulse	20	2	20	1 on 4 off	4	0:30	3:17	2:47
T-30		Wood	Pulse	20	2	20	2 on 6 off	4	0:30	2:48	2:18
T-31		Wood	Pulse	20	2	20	1 on 6 off	4	0:30	2:21	1:51
T-32		Wood	Pulse	20	2	20	2 on 5 off	4	0:30	3:17	2:47
T-33		Wood	Pulse	20	2	20	1 on 5 off	4	0:30	2:15	1:45
T-34	Feces Pulse	Feces	Pulse	30	3	20	1 on 4 off	4	1:00	3:35	2:35
T-35		Feces	Pulse	30	3	20	2 on 6 off	4	1:00	3:49	2:49

FULL SYSTEM NO AUGER			Test Type	Fuel Load	Fan Ramp	Pulse Set	Pulse Timing	Pulse Off	Pre-Fan	Time to Ign	Adj. Ign
T1	Fan Pulse	Wood	Full Pulse	30	Default	3.6	2 on 4 off	2	1:00	2:13	1:13
T2	Baseline	Wood	NA	30	Default	NA	NA	NA	1:00	2:16	1:16
T3-2	Fan Pulse	Wood	Full Pulse	30	Default	3.4	1 on 4 off	2	1:00	2:10	1:10
T4	dT 0.6	Wood	Full Pulse	30	Default	3.4	2 on 6 off	2	1:00	2:28	1:28
T5		Wood	Full Pulse	30	Default	3.4	2 on 4 off	2	1:00	1:59	0:59
T6	Feces Pulse	Feces	Full Pulse	30	Default	3.4	2 on 4 off	2	1:00	DNL	DNL
T7	dT 0.8	Wood	Full Pulse	30	Default	3.4	2 on 6 off	2	1:00	2:13	1:13
T8-2	dT 1.0	Wood	Full Pulse	30	Default	3.2	2 on 6 off	2	1:00	5:00	4:00
T9	Ign. Close Wait	Wood	Full Pulse	30	Default	3.4	1 on 4 off	2	1:00	4:46	3:46
T10	""	Wood	Full Pulse	30	Default	3.4	2 on 5 off	2	1:00	1:59	0:59
T11	Feces Pulse	Feces	Full Pulse	30	Default	3.4	2 on 5 off	2	1:00	4:27	3:27
T12	Feces Pulse	Feces	Full Pulse	30	Default	3.4	2 on 5 off	2	1:00	DNL	DNL
T13	Feces Pulse	Feces	Full Pulse	30	Default	3.4	2 on 5 off	2	1:00	DNL	DNL
T14	Wood dP Test	Wood	Full Pulse	30	Default	3.4	2 on 5 off	2	1:00	1:58	0:58
T15		Wood	Full Pulse	30	Default	3.4	2 on 5 off	2	1:00	DNL	DNL
T16		Wood	Full Pulse	30	Default	3.4	2 on 5 off	2	1:00	2:06	1:06
T17		Wood	Full Pulse	30	Default	3.4	2 on 5 off	2	1:00	1:50	0:50
T18	dP Baseline	Wood	Full Pulse	30	Default	3.4	2 on 5 off	2	1:00	2:39	1:39
T19-2	dP Baseline	Wood	Full Pulse	30	Default	3.4	2 on 5 off	2	1:00	2:14	1:14
T20		Wood	Full Pulse	30	Default	3.4	2 on 5 off	2	1:00	2:58	1:58
T21		Wood	Full Pulse	30	Default	3.4	2 on 5 off	2	1:00	2:09	1:09
T22		Wood	Full Pulse	30	Default	3.4	2 on 5 off	2	1:00	2:08	1:08
T23		Wood	Full Pulse	30	Default	3.4	2 on 5 off	2	1:00	1:57	0:57
T23-2		Wood	Full Pulse	30	Default	3.4	2 on 5 off	2	1:00	1:50	0:50
T24		Wood	Full Pulse	30	Default	3.4	2 on 5 off	2	1:00	1:48	0:48
T25		Wood	Full Pulse	30	Default	3.4	2 on 5 off	2	1:00	2:17	1:17
T26		Wood	Full Pulse	30	Default	3.4	2 on 5 off	2	1:00	1:39	0:39
T27		Wood	Full Pulse	30	Default	3.4	2 on 5 off	2	1:00	3:35	2:35
FL_T3	Full Flapper	Wood	Flap Pulse	30	Default	4.6	2 on 5 off	3.5	1:00	?	
FL_T4	Full Flapper	Wood	Flap Pulse	30	Default	4.6	2 on 5 off	3.5	1:00	?	
FL_T5	Full Flapper	Wood	Flap Pulse	30	Default	4.6	2 on 5 off	3.5	1:00	2:14	1:14
FL_T6	Full Flapper	Wood	Flap Pulse	30	Default	4.6	2 on 5 off	3.5	1:00	1:50	0:50
FL_T7	Feces Flapper	Feces	Flap Pulse	31.5	Default	4.6	2 on 5 off	3.5	1:00	2:10	1:10
FL_T8	Feces Flapper	Feces	Flap Pulse	30	Default	4.6	2 on 5 off	3.5	1:00	DNL	DNL
FL_T10	dT = 1.3	Wood	Flap Pulse	30	Default	4.6	2 on 5 off	3.5	1:00	2:22	1:22
FL_T11	dT = 1.3	Feces	Flap Pulse	30	Default	4.6	2 on 5 off	3.5	1:00	DNL	DNL
FL_T12	dT = 1.3	Feces	Flap Pulse	35	Default	4.6	2 on 5 off	3.5	1:00	DNL	DNL
FL_T13	dT = 1.3	Wood	Flap Pulse	25	Default	4.6	2 on 5 off	3.5	1:00	2:29	1:29
FL_T14	dT = 1.3	Feces	Flap Pulse	25	Default	4.6	2 on 5 off	3.5	1:00	DNL	DNL
FL_T15	Pulse = 4.7	Feces	Flap Pulse	30	Default	**4.7**	2 on 5 off	3.5	1:00	DNL	DNL
FL_T16	Pulse = 4.7	Feces	Flap Pulse	30	Default	**4.7**	**1 on 5 off**	3.5	1:00	DNL	DNL
FL_T17	Grind at 1:15	Wood	Flap Pulse	30	Default	4.6	2 on 5 off	3.5	1:00	1:40	0:40
FL_T18	Grind at 1:15	Feces	Flap Pulse	30	Default	4.6	2 on 5 off	3.5	1:00	DNL	DNL
FL_T19	Grind w/ Pulse?	Wood	Flap Pulse	30	Default	4.6	2 on 5 off	3.5	1:00	4:57	3:57
FL_T20	Grind w/ Pulse	Wood	Flap Pulse	30	Default	4.6	2 on 5 off	3.5	1:00	4:02	3:02
FL_T21	Grind w/ Pulse	Wood	Flap Pulse	30	Default	4.6	2 on 5 off	3.5	1:00	DNL	DNL
-	Baseline	Wood	Flap Pulse	30	Default	4.6	2 on 5 off	3.5	1:00	1:20	0:20

	Flap Grind Ramp Mods			Test Type	Fuel Load	Ramp	Pulse Set	Pulse Timing	Pulse Off	Starting dP	Pre-Fan	Time to Ign	Adj. Ign	Grind Start	Grind Int.	dT for Ign	dP at Ign
FL_T22	Rep T7	Feces	11/2	Flap Pulse	32	Default	4.6	2 on 5 off	3.5	0.22	1:00	7:29	6:29	3:00	1:00	1.3	0.22
FL_T23	Half Rev/min	Feces	11/2	Flap Pulse	40	Default	4.6	2 on 5 off	3.5	0.22	1:00	6:18	5:18	2:00	1:00	1.3	0.22
FL_T24	Half Rev/1.5 m	Feces	11/2	Flap Pulse	35	Default	4.6	2 on 5 off	3.5	0.22	1:00	6:28	5:28	2:30	1:30	1.3	0.22
FL_T25	Half Rev/2 m	Feces	11/2	Flap Pulse	30	Default	4.6	2 on 5 off	3.5	0.22	1:00	7:08	6:08	3:00	2:00	1.3	0.220
FL_T26	Add ramp	Feces	11/2	Flap Pulse	35	0.015	4.6	2 on 5 off	3.5	0.2	1:00	6:08	5:08	2:30	1:30	1.3	0.292
FL_T27	Rep T26	Feces	11/3	Flap Pulse	35	0.015	4.6	2 on 5 off	3.5	NA	1:00	DNL	DNL	1:00	1:30	1.3	NA
K9_T28	K9 Feces, dT 1.6	k9	11/7	Flap Pulse	35	0.01	4.6	2 on 5 off	3.5	0.2	1:00	2:41	1:41	None	None	1.6	0.227
K9_T29	k9 w/ grind	k9	11/7	Flap Pulse	35	0.01	4.6	2 on 5 off	3.5	0.2	1:00	2:35	1:35	2:30	1:30	1.6	0.226
K9_T30	Lower ramp	k9	11/7	Flap Pulse	35	0.008	4.6	2 on 5 off	3.5	0.2	1:00	2:16	1:16	2:30	1:30	1.6	0.218
K9_T31	Higher ramp	k9	11/7	Flap Pulse	35	0.012	4.6	2 on 5 off	3.5	0.2	1:00	5:31	4:31	2:30	1:30	1.6	0.266
T32	Wood	Wood	11/7	Flap Pulse	35	0.01	4.6	2 on 5 off	3.5	0.2	1:00	2:01	1:01	2:30	1:30	1.6	0.220
T33	Wood	Wood	11/16	Flap Pulse	30	0.01	4.6	2 on 5 off	3.5	0.2	0:30	1:48	1:18	2:30	1:30	1.6	0.218
T34	Wood	Wood	11/16	Flap Pulse	35	0.01	4.6	2 on 5 off	3.5	0.2	0:30	2:33	2:03	2:30	1:30	1.6	0.226
T35	Wood	Wood	11/16	Flap Pulse	35	0.015	4.6	2 on 5 off	3.5	0.2	0:30	1:50	1:20	2:30	1:30	1.6	0.228
FL_ T36	Low Ramp Hu	Feces	11/18	Flap Pulse	35	0.01	4.6	2 on 5 off	3.5	0.2	1:30	6:19	4:49	2:30	1:30	2	0.263

Taken from Data - Mass Flow Controlled System

Combustor Mode	Hole Sizes	Setpoint (SLPM)	Measured Airflow (SLPM)	Total Airflow (SLPM)	Airflow Ratio (Sec/Pri)
Micro Monfold - Steady State					
Primary Air	2mm * 10	13	12.94		
Secondary Air	4mm * 10	52	51.79	64.73	4.002318393

Dilution Ratio Calculations	Average Value - Indirect	Average Value - Direct	Hood Dilution Factor	*Hood Flowrate, LPM	Stove Flowrate, SLPM
CO2 %, 5/16	0.128927595	8.20086407	63.61	6011.000	79.1
CO PPM, 5/16	8.498277893	456.7115717	53.74	6011.000	111.8
CO2 %, 5/17	0.078959832	5.876836036	74.42817255	6011	80.8
		5.937756943	75.19971556	6011.000	79.9
CO PPM, 5/17	9.852631112	576.7210204	58.53472173	6011.000	102.7
		610.1969284	61.93238348	6011.000	97.1

Hazen Research, Inc.
4601 Indiana Street
Golden, CO 80403 USA
Tel: (303) 279-4501
Fax: (303) 278-1528

Date   October 21 2015
HRI Project   009-980
HRI Series No. J158/15-1
Date Rec'd.   10/14/15
Cust. P.O.#

CSU Powerhouse
Max Flagg
430 North College Avenue
Fort Collins, Colorado 80524

Sample Identification
HU Run 1

Reporting Basis >	As Rec'd	Dry	Air Dry
Proximate (%)			
Moisture	3.98	0.00	3.98
Ash	14.33	14.92	14.33
Volatile			
Fixed C			
Total	_____	_____	_____
Sulfur	0.950	0.989	0.950
Btu/lb (HHV)	9218	9601	9218
Btu/lb (LHV)	8574	8972	
MMF Btu/lb	10918	11461	
MAF Btu/lb		11285	
Ultimate (%)			
Moisture	3.98	0.00	3.98
Carbon	48.61	50.62	48.61
Hydrogen	6.51	6.78	6.51
Nitrogen	4.60	4.79	4.60
Sulfur	0.95	0.99	0.95
Ash	14.33	14.92	14.33
Oxygen*	21.02	21.90	21.02
Total	100.00	100.00	100.00
Chlorine**			

Air Dry Loss (%)
Forms of Sulfur, as S, (%)

Sulfate		
Pyritic		
Organic	_____	_____
Total	0.95	0.99

Water Soluble Alkalies (%)

Na20
K20

Lb. Alkali Oxide/MM Btu=
Lb. Ash/MM Btu=   15.54
Lb. SO2/MM Btu=   2.06
Lb. Cl/MM Btu=
As Rec'd. Sp.Gr.=
Free Swelling Index=
F-Factor(dry),DSCF/MM Btu= 9,720

Report Prepared By:

Gerard H. Cunningham
Fuels Laboratory Supervisor

* Oxygen by Difference.
** Not usually reported as part of the ultimate analysis.

An Employee-Owned Company

Hazen Research, Inc.
4601 Indiana Street
Golden, CO 80403 USA
Tel: (303) 279-4501
Fax: (303) 278-1528

Date   October 21 2015
HRI Project   009-980
HRI Series No.   J158/15-1R
Date Rec'd.   10/14/15
Cust. P.O.#

CSU Powerhouse
Max Flagg
430 North College Avenue
Fort Collins, Colorado 80524

Sample Identification
HU Run 2

-

Reporting Basis >	As Rec'd	Dry	Air Dry
Proximate (%)			
Moisture	3.79	0.00	3.79
Ash	14.17	14.73	14.17
Volatile			
Fixed C	————	————	————
Total			
Sulfur	0.859	0.893	0.859
Btu/lb (HHV)	9247	9611	9247
Btu/lb (LHV)	8582	8961	
MMF Btu/lb	10928	11443	
MAF Btu/lb		11271	
Ultimate (%)			
Moisture	3.79	0.00	3.79
Carbon	49.08	51.01	49.08
Hydrogen	6.75	7.01	6.75
Nitrogen	4.61	4.79	4.61
Sulfur	0.86	0.89	0.86
Ash	14.17	14.73	14.17
Oxygen*	20.74	21.57	20.74
Total	100.00	100.00	100.00

Chlorine**

Air Dry Loss (%)
Forms of Sulfur, as S, (%)

	As Rec'd	Dry
Sulfate		
Pyritic		
Organic	————	————
Total	0.86	0.89

Water Soluble Alkalies (%)
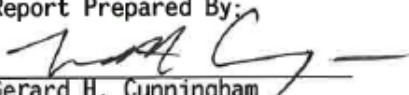
Na20
K20

Lb. Alkali Oxide/MM Btu=
Lb. Ash/MM Btu=   15.32
Lb. S02/MM Btu=   1.86
Lb. Cl/MM Btu=
As Rec'd. Sp.Gr.=
Free Swelling Index=
F-Factor(dry),DSCF/MM Btu=   9,868

Report Prepared By:

Gerard H. Cunningham
Fuels Laboratory Supervisor

* Oxygen by Difference.
** Not usually reported as part of the ultimate analysis.

An Employee-Owned Company

77

Date   October 21 2015
HRI Project   009-980
HRI Series No. J158/15-2
Date Rec'd.   10/14/15
Cust. P.O.#

CSU Powerhouse
Max Flagg
430 North College Avenue
Fort Collins, Colorado 80524

Sample Identification
K9 Run 1

-

Reporting Basis >	As Rec'd	Dry	Air Dry
Proximate (%)			
Moisture	3.22	0.00	3.22
Ash	26.06	26.93	26.06
Volatile			
Fixed C			
Total	———	———	———
Sulfur	0.621	0.642	0.621
Btu/lb (HHV)	6377	6589	6377
Btu/lb (LHV)	5882	6112	
MMF Btu/lb	8874	9293	
MAF Btu/lb		9018	
Ultimate (%)			
Moisture	3.22	0.00	3.22
Carbon	36.22	37.43	36.22
Hydrogen	4.98	5.15	4.98
Nitrogen	3.98	4.11	3.98
Sulfur	0.62	0.64	0.62
Ash	26.06	26.93	26.06
Oxygen*	24.92	25.74	24.92
Total	100.00	100.00	100.00
Chlorine**			

Air Dry Loss (%)
Forms of Sulfur, as S, (%)

	As Rec'd	Dry
Sulfate		
Pyritic		
Organic	———	———
Total	0.62	0.64

Lb. Alkali Oxide/MM Btu=
Lb. Ash/MM Btu=   40.86
Lb. SO2/MM Btu=   1.95
Lb. Cl/MM Btu=
As Rec'd. Sp.Gr.=
Free Swelling Index=
F-Factor(dry),DSCF/MM Btu= 9,877

Water Soluble Alkalies (%)

Na20
K20

Report Prepared By:

Gerard H. Cunningham
Fuels Laboratory Supervisor

* Oxygen by Difference.
** Not usually reported as part of the ultimate analysis.

Hazen Research, Inc.
4601 Indiana Street
Golden, CO 80403 USA
Tel: (303) 279-4501
Fax: (303) 278-1528

CSU Powerhouse
Max Flagg
430 North College Avenue
Fort Collins, Colorado 80524

Sample Identification
K9 Run 2

-

Reporting Basis >	As Rec'd	Dry	Air Dry
Proximate (%)			
Moisture	3.28	0.00	3.28
Ash	29.11	30.10	29.11
Volatile			
Fixed C			
Total	————	————	————
Sulfur	0.680	0.703	0.680
Btu/lb (HHV)	6291	6504	6291
Btu/lb (LHV)	5791	6023	
MMF Btu/lb	9176	9640	
MAF Btu/lb		9305	
Ultimate (%)			
Moisture	3.28	0.00	3.28
Carbon	36.77	38.02	36.77
Hydrogen	5.02	5.19	5.02
Nitrogen	4.07	4.21	4.07
Sulfur	0.68	0.70	0.68
Ash	29.11	30.10	29.11
Oxygen*	21.07	21.78	21.07
Total	100.00	100.00	100.00

Chlorine**

Air Dry Loss (%)
Forms of Sulfur, as S, (%)

Sulfate		
Pyritic		
Organic	————	————
Total	0.68	0.70

Water Soluble Alkalies (%)

Na2O
K2O

Lb. Alkali Oxide/MM Btu=
Lb. Ash/MM Btu=   46.27
Lb. SO2/MM Btu=   2.16
Lb. Cl/MM Btu=
As Rec'd. Sp.Gr.=
Free Swelling Index=
F-Factor(dry),DSCF/MM Btu= 10,461

Report Prepared By:

Gerard H. Cunningham
Fuels Laboratory Supervisor

* Oxygen by Difference.
** Not usually reported as part of the ultimate analysis.

An Employee-Owned Company

CSU Powerhouse
Max Flagge
430 N College Ave
Fort Collins, CO 80524

Date   March 1, 2017
HRI Project   009-976
HRI Series No.   B49/17-1
Date Rec'd.   02/17/17
Cust. P.O.#

Sample Identification
HU-RTI

Reporting Basis >	As Rec'd	Dry	Air Dry
Proximate (%)			
Moisture	34.47	0.00	2.99
Ash	8.70	13.28	12.88
Volatile	48.55	74.09	71.87
Fixed C	8.28	12.64	12.26
Total	100.00	100.00	100.00
Sulfur	0.350	0.534	0.518
Btu/lb (HHV)	6077	9274	8997
Btu/lb (LHV)	5311	8646	
MMF Btu/lb	6702	10832	
MAF Btu/lb		10694	
Ultimate (%)			
Moisture	34.47	0.00	2.99
Carbon	38.23	58.34	56.60
Hydrogen	4.44	6.78	6.58
Nitrogen	3.43	5.24	5.08
Sulfur	0.35	0.53	0.52
Ash	8.70	13.28	12.88
Oxygen*	10.37	15.83	15.35
Total	100.00	100.00	100.00
Chlorine**			

Air Dry Loss (%)   32.45
Forms of Sulfur, as S, (%)

  Sulfate
  Pyritic
  Organic   _____   _____

  Total   0.35   0.53

Water Soluble Alkalies (%)

  Na2O
  K2O

Lb. Alkali Oxide/MM Btu =
Lb. Ash/MM Btu=   14.30
Lb. SO2/MM Btu=   1.15
Lb. Cl/MM Btu=
As Rec'd. Sp. Gr.=
Free Swelling Index=
F-Factor(dry),DSCF/MM Btu=   11,613

Report Prepared By:

Mark A. Pugh
Fuel Laboratory Manager

* Oxygen by difference
** Not usually reported as part of the ultimate analysis.

Hazen Research, Inc.
4601 Indiana Street
Golden, CO 80403 USA
Tel: (303) 279-4501
Fax: (303) 278-1528

CSU Powerhouse
Max Flagge
430 N College Ave
Fort Collins, CO 80524

Date: March 1, 2017
HRI Project: 009-976
HRI Series No. B49/17-2
Date Rec'd. 02/17/17
Cust. P.O.#

Sample Identification
HU-INDIA

Reporting Basis >	As Rec'd	Dry	Air Dry
Proximate (%)			
Moisture	3.64	0.00	3.64
Ash	11.80	12.25	11.80
Volatile	67.98	70.55	67.98
Fixed C	16.58	17.21	16.58
Total	100.00	100.00	100.00
Sulfur	0.438	0.455	0.438
Btu/lb (HHV)	8341	8656	8341
Btu/lb (LHV)	7763	8096	
MMF Btu/lb	9560	9977	
MAF Btu/lb		9864	
Ultimate (%)			
Moisture	3.64	0.00	3.64
Carbon	54.11	56.15	54.11
Hydrogen	5.82	6.04	5.82
Nitrogen	4.61	4.78	4.61
Sulfur	0.44	0.45	0.44
Ash	11.80	12.25	11.80
Oxygen*	19.58	20.32	19.58
Total	100.00	100.00	100.00
Chlorine**			
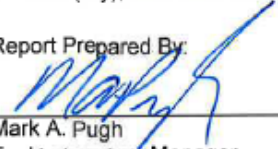
Air Dry Loss (%)	0	
Forms of Sulfur, as S, (%)		
Sulfate		
Pyritic		
Organic	___	___
Total	0.44	0.45

Water Soluble Alkalies (%)

Na2O
K2O

Lb. Alkali Oxide/MM Btu =
Lb. Ash/MM Btu= 14.13
Lb. SO2/MM Btu= 1.05
Lb. Cl/MM Btu=
As Rec'd. Sp. Gr.=
Free Swelling Index=
F-Factor(dry),DSCF/MM Btu= 11,495
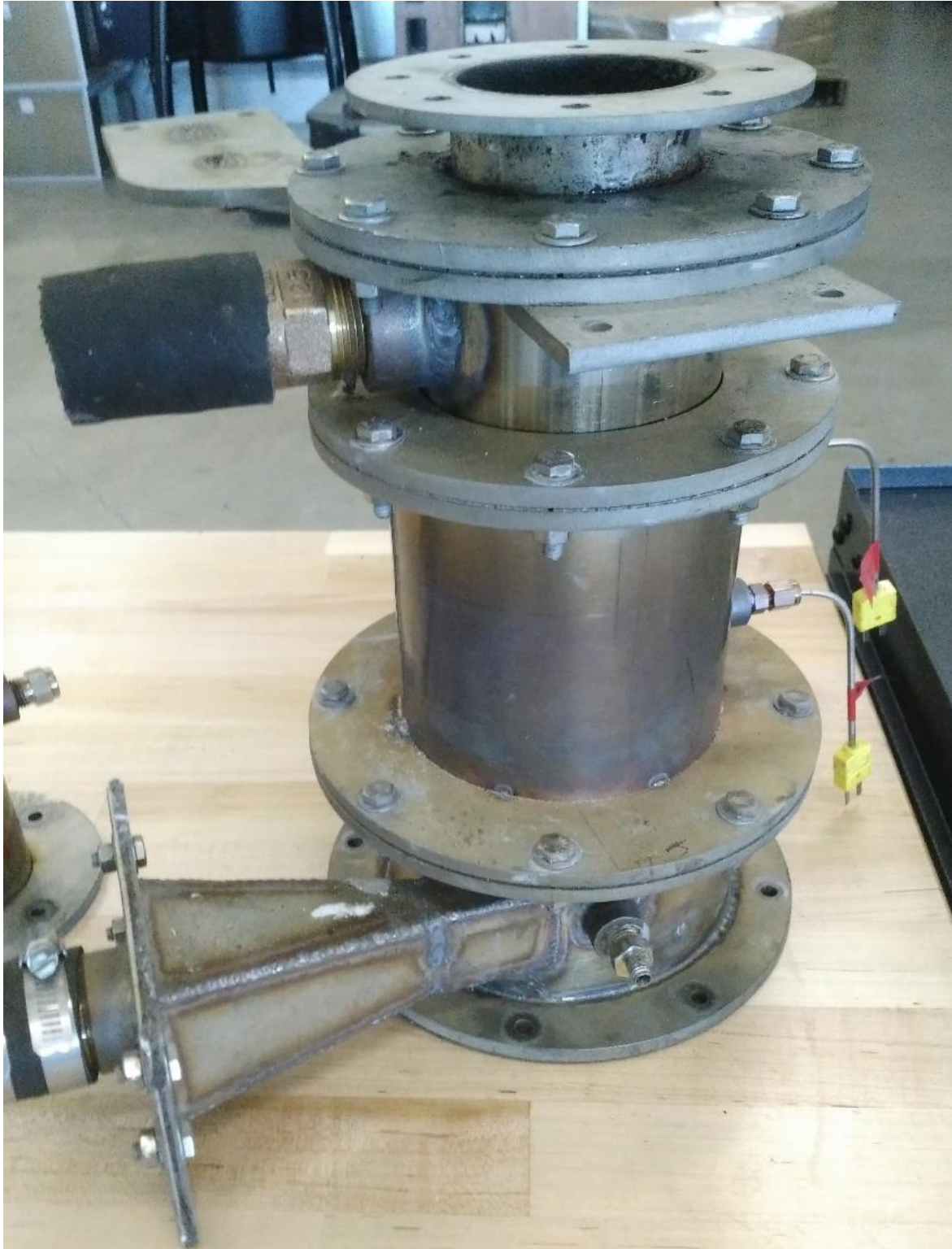
Report Prepared By:

Mark A. Pugh
Fuel Laboratory Manager

* Oxygen by difference
** Not usually reported as part of the ultimate analysis.

Downdraft Combustor

Flippable Micro Combustor

Updraft Micro Combustor V2

Updraft Micro Combustor V3

Micro Monofold Combustor

APPENDIX F – EXHAUST GAS CALCULATIONS

This work was created in conjunction with Kyle Greer

```matlab
clear; clc;
%% Inputs

% phi = 1;
% m_dot_fuel = 500/3600/1000; %kg/s
% T = 800+273.15; LHV = 0;
%
% % Input mass fractions
% mf.C = 50.62;
% mf.H = 6.78;
% mf.N = 4.79;
% mf.O = 21.9;
% mf.S = 0.99;
% mf.ash = 14.92;


[mf, phi, m_dot_fuel, T, LHV, mass_based] = func_GUI_inputs;

%% Constants
P = (12.3/14.6959)*101325; %Pa, taken to be pressure in Fort Collins
Ru = 8315; % J/kmol-k
%Molar Masses, kg/kmol
MW.C = 12.011;
MW.H = 1.0079;
MW.O = 15.999;
MW.N = 14.0067;
MW.S = 32.065;
MW.air = 28.9645;
MW.CO2 = MW.C + 2*MW.O;
MW.H2O = MW.H*2 + MW.O;
MW.N2 = 2*MW.N;
MW.SO2 = MW.S + 2*MW.O;
MW.O2 = 2*MW.O;

%% Convert Mass-based to moles
if mass_based == 1
    % Convert to ashless mass fraction
    Y.ashless = mf.C + mf.H + mf.N + mf.O + mf.S;
    Y.C = mf.C/Y.ashless;
    Y.H = mf.H/Y.ashless;
    Y.O = mf.O/Y.ashless;
    Y.N = mf.N/Y.ashless;
    Y.S = mf.S/Y.ashless;

    % Convert to molar fuel chemistry CaHbOcNdSe

    MW.fuel = 1/(Y.C/MW.C + Y.H/MW.H + Y.O/MW.O + Y.N/MW.N + Y.S/MW.S); %
ashless fuel, kg/kmol, EQ 2.12b

    % mole fractions of fuel constituents, eq 2.11b
    a = Y.C*MW.fuel/MW.C;
    b = Y.H*MW.fuel/MW.H;
```

```matlab
    c = Y.O*MW.fuel/MW.O;
    d = Y.N*MW.fuel/MW.N;
    e = Y.S*MW.fuel/MW.S;

else % if inputs were already molar-based
    a = mf.C;
    b = mf.H;
    c = mf.O;
    d = mf.N;
    e = mf.S;

    MW.fuel = a*MW.C + b*MW.H + c*MW.O + d*MW.N + e*MW.S;
end

%% Combustion Equation: CaHbOcNdSe + A(O2 +3.76N2) --> aCO2 + b/2H20 + (d/2 +
3.76A)N2 + eSO2 + fO2

A_s = a + b/4 + e - c/2; %Stoich 'A'
A = A_s./phi; % Eq 2.33: N_air_act = N_air_stoich/phi
f = A - A_s; % moles excess air
N_prod = a + b/2 + (d/2 + 3.76*A) + e + f;

%% Flow Rate Calcs

AF_stoic = 4.76 * A_s * MW.air/MW.fuel; %EQ 2.32
AF_act = AF_stoic./phi; % Air:Fuel Flowrate

m_dot_ashless = (1 - mf.ash/100)*m_dot_fuel;

m_dot_hr = m_dot_fuel*3600000;

m_dot_air = AF_act * m_dot_ashless; % kg/s

m_dot_exhaust = m_dot_air + m_dot_ashless; %kg/s

%% Molar Fractions Exhaust
mol_frac.co2 = a./N_prod;
mol_frac.h2o = (b/2)./N_prod;
mol_frac.n2 = (d/2 + 3.76.*A)./N_prod;
mol_frac.so2 = e./N_prod;
mol_frac.o2 = f./N_prod;

%% Exhaust Ideal Gas, Flowrate Calc
P_i = [P*mol_frac.co2, P*mol_frac.h2o, P*mol_frac.n2, P*mol_frac.so2,
P*mol_frac.o2]; %Pa
for idx = 1:numel(T)
    rho_i = (1./(T(idx).*Ru)).*[P_i(1).*MW.CO2, P_i(2).*MW.H2O,
P_i(3).*MW.N2, P_i(4).*MW.SO2, P_i(5).*MW.O2];  %kg/m3
    rho_tot(idx) = sum(rho_i); %kg/m3
end

Q_exhaust = 60000.*m_dot_exhaust./rho_tot; %L/min
SLPM_ex = Q_exhaust.*(P./101325.353).*(293.15./T);
```

Average fuel feedrate = 775 g/hr

Exhaust temp = 800C, phi = 1

Fuel = Dehydrated Human Feces from RTI (North Carolina)

Exhaust Flow vs. $\dot{m}_{Fuel}$ (g/hr)

Exhaust Flow vs. $T_{Exhaust}$